Ca isotopic analysis of laser-cut microsamples of (bio) apatite without chemical purification

Qiong Li[1*], *Matthew Thirlwall*[1], *Wolfgang Müller*[1]

[1] *Earth Sciences Department, Royal Holloway University of London, Egham Hill, Egham, UK, TW20 0EX*

**Corresponding author, email: qiong.li@rhul.ac.uk*

Abstract

We report methodological innovations and initial applications to retrieve Ca isotopic ($\delta^{44/40}$Ca) compositions of bioapatite at high spatial resolution. Advances over previous TIMS methods include: 1) Laser-microsampling via 20 µm wide laser-cut polygons followed by extraction of µg-sized bioapatite fragments, 2) no ion exchange chromatography after sample dissolution,3) TIMS analysis using a 10^{10} Ω resistor for ^{40}Ca, 4) parafilm-dam loading that significantly restricts in-run Ca isotope fractionation..

Identical internally-normalized Ca isotopic ratios are achieved for natural calcite, apatite and bone meal SRM 1486 without chemical separation, suggesting no need of chemical purification for TIMS Ca isotopic analysis of such materials. Our ^{42}Ca-^{48}Ca double spike (DS) corrected $\delta^{44/40}$Ca values of standard solutions HPS_{new}, Fisher 07 and bone meal SRM 1486 are 0.70 ± 0.18 ‰, 1.03 ± 0.20 ‰, and -1.03 ± 0.19 ‰ (2SD), relative to SRM 915a, all well in line with published data and validating our DS-correction technique. Solutions prepared from both laser-cut and non-laser cut Durango apatite have similar $\delta^{44/40}$Ca values (0.70 ± 0.17 ‰, 2SD), suggesting no resolvable Ca isotope fractionation effect induced by the laser-cutting process.

An initial $\delta^{44/40}$Ca profile of human enamel apatite, laser-sampled in the growth direction from a third molar of a modern female, reveals a 0.73 ‰ decrease that coincides with the onset of her menstruation. This indicates a relationship between physiological change and $\delta^{44/40}$Ca excursion, and raises the need for proper evaluation of physiological effects on Ca isotopes before reliable environmental signals can be extracted from the large Ca-isotope variability previously observed in fossil skeletal tissues.

We also investigated the potential for Ca isotopic analysis using both solution and laser ablation (LA) sample input to an IsoProbe MC-ICPMS. While the use of a collision cell

almost completely removes $^{40}Ar^{+}$ interference on $^{40}Ca^{+}$, partially-resolved hydrocarbon interferences result in only ~30% useable peakflats, that potentially cause problems with peak jumping needed for analysis of ^{46}Ca and ^{48}Ca. Further, it is difficult to correct for Ti isobaric interferences so that analysis without chemical separation is not practical. In-situ direct Ca isotope analysis of natural calcite, aragonite and apatite by LA-MC-ICPMS shows substantial matrix sensitivity, and therefore requires close matrix matching.

Keywords: Ca isotopes, enamel apatite, TIMS, (LA-) MC-ICPMS, double spike, Laser-microsampling

1 Introduction

Precise Ca isotopic analysis was established using modern mass spectrometers and the double spike mass fractionation correction technique by Russell (1978). Since then a large amount of Ca-isotope work has been focused on the global Ca cycle (e.g. Zhu and Macdougall, 1998; Schmitt et al., 2003; Tipper et al., 2006); and palaeoceanographic reconstruction using marine skeletal carbonates (e.g. Nagler et al., 2000; Gussone et al., 2004; Heuser et al., 2005; Hippler et al., 2006; Farkas et al., 2007; Brazier et al., 2015). Ca isotopic variations in biological samples hold vital clues of Ca pathways during bio-mineralisation and metabolism. Some marine bone apatite and calcium carbonate suggest a Ca trophic level effect, namely a lowering in $\delta^{44/40}Ca$ of ~1 ‰ per trophic level in marine environment (Skulan et al., 1997; Clementz et al., 2003; DePaolo, 2004), but such effect is not convincing between herbivores and carnivores, and at the higher end of the food chain in terrestrial environment (Chu et al., 2006; Reynard et al., 2010; Heuser et al., 2011). The larger Ca-isotope variability but lower delta values in human bones relative to fauna at some archaeological sites may result from more complicated processes (e.g. Ca metabolism) than trophic level effects (Skulan and DePaolo, 1999; Reynard et al., 2010). A comprehensive understanding of physiological and environmental controls on Ca isotope fractionation in different skeletal tissues will allow us to reliably extract the environmental signals potentially carried by Ca-isotopes. Improvements in Ca-isotope methodology will help to reveal further details of natural Ca isotopic variabilities and hence are critical to assess fully the potential of using Ca isotopes as a geochemical proxy.

Ca isotopic ratios have conventionally been measured by TIMS due to its high sensitivity and an external precision of ~ 0.15 – 0.30 ‰ (2SD) in $\delta^{44/40}Ca$ has been achieved using the double spike (commonly ^{42}Ca – ^{48}Ca or ^{43}Ca – ^{48}Ca DS) technique (e.g. Russell et al., 1978;

Skulan et al., 1997; Heuser et al., 2002; Huang et al., 2012; Lehn and Jacobson, 2015), through recent Ca isotope analyses ($\delta^{44/40}$Ca) using an optimized ^{42}Ca – ^{43}Ca DS showed an external 2SD of 0.04 ‰ (Lehn et al., 2013). Such TIMS analyses are accurate and precise, but have required prolonged sample preparation and running time. An alternative, more rapid approach using MC-ICPMS was then developed with Ca isotopic data corrected for mass bias using the standard-sample bracketing technique (Halicz et al., 1999; Wieser et al., 2004; Chu et al., 2006; Hirata et al., 2008; Reynard et al., 2010). However, compared with TIMS, Ca work by MC-ICPMS faces a big challenge: interference of Ar-species ions from the plasma on Ca isotopes (e.g. $^{40}Ar^{+}$ on $^{40}Ca^{+}$). Most hydrocarbon interferences, even those on minor Ca isotopes are resolvable at medium to high resolution on MC-ICPMS, though.

Earlier Ca-work by MC-ICPMS avoided this issue by not measuring ^{40}Ca, so reporting data as $\delta^{44/42}$Ca with 0.1 – 0.2 ‰ (2SD) using sample-standard bracketing (Halicz et al., 1999; Wieser et al., 2004). This is equivalent to 0.2 – 0.4 ‰ (2SD) on $\delta^{44/40}$Ca. Due to $^{88}Sr^{2+}$ interference on ^{44}Ca, the removal of Sr is very important for MC-ICPMS analysis of Ca isotopes. Introducing sample as a dry aerosol to the plasma and chemical purification prior to measurement, have been found to contribute to minimizing isobaric interferences and systematic drift due to matrix differences (Halicz et al., 1999; Wieser et al., 2004; Chu et al., 2006; Reynard et al., 2010, 2011). In practice, the one-step chemical separation of Ca from Sr and the rest of the matrix (Wieser et al., 2004) requires columns with extreme length/diameter ratio ($\geq$ 50), making both separation and column cleaning very slow and difficult. Although some argue that the use of Sr-specific resin only to remove the Sr ions from carbonate solutions is sufficient to avoid interference and matrix effects (Brazier et al., 2015), the difficulty of the chemical purification for MC-ICPMS depends on the complexity of samples (Tipper et al., 2008). The two column procedure (e.g. Chu et al., 2006; Hirata et al., 2008; Reynard et al., 2010), or the three-step separation (Tipper et al., 2008; Tacail et al., 2014), or even the four-step purification scheme (Schiller. et al., 2012), which involve the step separation of Ca from Sr and the rest of the matrix, is costly and time-consuming. More importantly, Ca isotope fractionation can occur during column chemistry if Ca recovery is not nearly 100 % (Russell and Papanastassiou, 1978). It is therefore desirable to minimize chemical purification to avoid biasing Ca isotopic measurements.

Another strategy is to make direct $\delta^{44/40}$Ca measurements by MC-ICPMS using the cold plasma technique (Fietzke et al., 2004) or using reaction/collision cells to eliminate ^{40}Ar ions (Palacz, 2004). However, the cold plasma (500W) technique does not completely eliminate

$^{40}Ar^{+}$ and requires careful sample matrix matching to minimize the changes in sensitivity and mass bias due to matrix changes (Fietzke et al., 2004). On the other hand, a MC-ICPMS, such as the GV Instrument IsoProbe can theoretically allow precise measurements of ^{40}Ca because it has a collision cell where a small flow of H_2 is introduced to neutralize $^{40}Ar^{+}$ via charge transfer (Palacz, 2004). However, such mass spectrometers are discontinued, so not widely available any more.

Calcium isotope data by MC-ICPMS are often corrected for mass bias using a standard-sample bracketing technique that works on the assumption that sample and bracketing standards experience the same mass bias and that mass fractionation during an analysis is fairly constant. However, this assumption may not always hold true because subtle variations in the matrix between samples and standards can cause change in the instrumental sensitivity and mass bias.

As an alternative to the standard-sample bracketing technique, the standard addition method has recently been used to correct MC-ICP-MS Ca isotopic data (Tipper et al., 2008). This method is designed to analyse solutions with significantly different matrix to the standard matrix. Despite the advantage in getting high precision and accuracy (e.g. seawater $\delta^{44/42}Ca$ of 0.93 ± 0.05 ‰, 2SD, n = 7, by Tipper et al. (2008)), this method is very complicated and time-consuming. The success of this technique requires correct performance in each analytical step. Such a complexity in standard addition technique limits its wide application in MC-ICPMS analysis for stable isotopes.

Others proposed to take advantage of both TIMS and high resolution (HR) MC-ICPMS to obtain precise and accurate data on a complete range of Ca isotopes for a single sample, with ^{42}Ca to ^{48}Ca measured on HR MC-ICPMS and ^{40}Ca to ^{44}Ca on TIMS (Schiller et al., 2012). This technique is particularly useful for determining mass-independent effects on small Ca isotopes (e.g. ^{46}Ca) because HR MC-ICPMS (such as Neptune plus) can produce long-lasting stable ion beams for even minor Ca isotopes.

While significant efforts have been made in order to improve the precision and accuracy of Ca isotopic data by MC-ICPMS, less has been done to improve the efficiency of TIMS Ca isotopic analysis, in part because DS-TIMS analysis is a well-established method. In this study, we first report high-precision TIMS Ca isotopic measurements (^{40}Ca, ^{42}Ca, ^{43}Ca, ^{44}Ca and ^{48}Ca) of five different Ca isotopic standards and tooth enamel (bio-apatite), using the following improved techniques: 1) laser-cutting for high-precision microsampling; 2)

simplified sample preparation with no ion exchange chromatography; 3) parafilm-dam loading technique that profoundly reduces the in-run fractionation and prevents mixing/unmixing between different Ca reservoirs on a Re-filament; 4) 10^{10} Ω resistor on the collector that measures ^{40}Ca, allowing good signals on small Ca isotopes ($^{42}Ca = 1.5\times10^{-3}$ nA and $^{48}Ca = 0.5\times10^{-3}$ nA); 5) ^{42}Ca–^{48}Ca double spike and a Matlab model for mass fractionation correction. We also present the first microsampled Ca isotope profile in modern human tooth enamel to evaluate the physiological controls on Ca isotopes. Data from our study should help to interpret the large Ca-isotope variability indicated in bones at some archaeological sites (Reynard et al., 2010).

2 Materials and method development

2.1 Tooth enamel sample and standards

A third molar (named CLW2) of a Chinese female that mineralized during her adolescent life (approximately 11-14yrs) was donated and made into a thick section with a thickness of 80 μm. The thick section was made using Crystalbond Adhesive (509 Clear) with a low melting point (121°C) and soluble in acetone, allowing the extraction of laser-cut enamel microsamples via gentle heating.

Five Ca isotopic standards were analysed in this study, including one primary standard SRM 915b, and four secondary standards: (1) HPS_{new} (high purity Ca solution, lot no. 1213234) from Greyhound Chromatography Ltd; (2) Fisher07 (code J/8010/08) from Fisher Scientific Ltd; (3) SRM 1486 (bone meal) and (4) Durango apatite, a fission track age standard from Durango City, Durango, Mexico (Young et al., 1969; McDowell et al., 2005). HPS_{new} and Fisher07 were purchased as calcite solutions (Ca concentration: 1000 mg/l). Weighed SRM 915b (powder) and Durango apatite (fragments) were dissolved in concentrated HNO_3 and heated to dryness, followed with dissolution in 18.2 MΩ·cm H_2O. SRM 1486 (bone meal) was first treated with concentrated HNO_3 and H_2O_2 to remove the collagen, and then heated to dryness and made into Ca solution with 18.2 MΩ·cm H_2O. All the standard solutions have a Ca concentration of 1000 ± 3 mg/l and analysed for Ca isotopes by TIMS without chemical purification.

2.2 Laser micro-sampling of (bio) apatite

A RESOlution M-50 193 nm laser-ablation system (Muller et al., 2009) at Royal Holloway University of London (RHUL) was used to cut enamel microsamples along the

159 enamel-dentine junction (EDJ) of the tooth section. The laser operating conditions were 20
160 Hz repetition rate, ~ 9 J/cm^2 laser fluence, 20 μm spot size, 20 μm/sec scan speed and 20
161 passes to ensure complete cutting through the enamel. . The cutting strategy of the modern
162 wisdom tooth CLW2 is shown in Fig. 1. Two long laser tracks (blue line) were placed along
163 the enamel-dentine junction (EDJ, white line) with an offset of 180 μm, and short laser tracks
164 (blue lines) across these two lines at an interval of 500 μm. It allowed the retrieval of
165 rectangular-shaped microsamples (180 ×500 μm, 10 – 20 μg apatite each) corresponding to a
166 discrete interval of growth. It is a trade-off between microsampling resolution and reasonable
167 sample size for separation, cleaning and Ca isotopic analysis. After laser cutting, the thick
168 section was placed on a ceramic tile preheated at ~ 120 °C for 5-10 mins, which was then
169 examined under a binocular microscope. The mild heat from the tile softened the crystal bond
170 for ~ 5 mins, allowing microsamples to be transferred to individually pre-cleaned 3ml PFA
171 vials filled with acetone using fine tweezers or needles. Crystalbond Adhesive was removed
172 ultrasonically in acetone, and microsamples rinsed with H_2O several times and left to dry in a
173 clean hood. They were then dissolved in 300 μl concentrated HNO_3 in new pre-cleaned vials
174 and evaporated to dryness. A few μl 18.2 MΩ·cm H_2O were added to make 1 μg/μl Ca
175 solutions. An aliquot of 2 μl solution (containing 2 μg Ca) from each vial was mixed with
176 4.62 μl DS solution (80.9 μg/ml Ca) and loaded on a single degassed Re-filament for TIMS
177 analysis.

178 In order to test for any laser-cutting induced mass fractionation on Ca isotopes, Durango
179 apatite solutions, prepared using two separate methods, were analysed by TIMS. The first
180 solution (Ca = 1000 mg/l) was made by direct dissolution of a clean piece of weighed
181 Durango apatite. The subsequent solutions were prepared using the Durango pieces (namely
182 A1, A2, B1, B2 & C) that were laser-cut from a 100 μm thick section (Fig. 2), following the
183 same laser settings as for tooth enamel. Areas A1 and A2 were additionally covered by laser
184 tracks to magnify any potential laser-related Ca mass fractionation. The apatite pieces were
185 separated, cleaned and dissolved in the same way as tooth enamel microsamples before being
186 diluted to 1000 mg/l Ca nitrate solution with 18.2 MΩ·cm H_2O.

187 **2.3 Improved TIMS loading technique**

188 Loading was performed using a parafilm dam technique that has been applied for TIMS
189 loading by Holmden and Bélanger (2010), Lehn et al. (2013) and Lehn and Jacobson (2015).
190 A pair of parafilm dams with a distance of ~ 1 mm between them was built on to the centre of

each out-gassed single Re filament at 0.5 A. About 1 µl of TaF_5-H_3PO_4 emitter was then loaded between the dams before small increments of sample solution (~ 2 µg Ca in total) were loaded. The surface tension that the parafilm dams created held the emitter – sample mixture within the dams and therefore minimized sample spread to ≤ 1 mm. Once the loaded sample was dry, the current was gradually brought up to 2.2 – 2.3 A, at which most filaments glowed.

The loading blank of our approach is ~ 1 ng, negligible to the 2 µg Ca load. This approach effectively reduces the in-run fractionation of $^{40}Ca/^{44}Ca$ (measured) on single Re-filaments to as low as 0.7 % and no higher than 5 % in rare cases when the spread reaches ⅓ of the filament length (3-4 mm). For comparison, regular loading on single Re-filaments without parafilm dams in our study can spread from ⅓ to over ½ of the filaments, and tends to have an in-run fractionation of up to 9 % for measured $^{40}Ca/^{44}Ca$ ratios (Supplementary material A). With such a large range of fractionation, there is a possibility of mixing between Ca reservoirs with different fractionation history on the filament (Hart and Zindler, 1989). Despite the fact that triple Re-filaments have extremely small in-run isotope fractionation on Ca (~ 0.5 %, Huang et al., 2012), they require a prolonged filament warm-up procedure and fail easily. The parafilm loading on single Re-filaments is therefore a faster and simpler method for TIMS Ca isotopic analysis.

2.4 TIMS running conditions for Ca isotopic analysis

Ca isotopic ratios were measured using a IsotopX Phoenix-X62 TIMS at RHUL. Ca isotopes were measured in a static mode in two sequences with ^{40}Ca, ^{42}Ca, ^{43}Ca and ^{44}Ca collected in the first sequence, and ^{44}Ca, ^{46}Ca and ^{48}Ca in the second sequence (Supplementary material B). ^{41}K was measured to correct for any ^{40}K interference on ^{40}Ca, using the $^{40}K/^{41}K$ ratio of 0.0017384, but ^{40}K correction on ^{40}Ca was only 1 – 2 ppm. No doubly charged $^{87}Sr^{2+}$ or Ti ions were observed in our samples. With 1 – 2 µg Ca load, ^{40}Ca signal was constrained to a 1.5 – 2 nA window using a $10^{10}\Omega$ resistor on collector L5. Each sample run contains 14 blocks, 10 cycles each, with 10s integration time for each peak. Baselines were measured individually in each cycle at mass 47.5 with 10s integration time before and after each peak.

2.5 Double spike calibration and mass fractionation correction algorithm

A ^{42}Ca–^{48}Ca double spike (DS) solution was prepared from two single isotopically enriched carbonates, Ca42-LO (^{42}Ca: 94.4 %) and Ca48-SM (^{48}Ca: 97.8 %) from Oak Ridge

National Laboratory (ORNL, USA). These were dissolved in 2 % HNO_3, and mixed in such a way that the $^{48}Ca/^{42}Ca$ ratio (~1.496) in the double spike solution is very close to the optimal value of 1.569 for a similar ORNL ^{42}Ca–^{48}Ca double spike of Rudge et al., (2009), with the objective of minimizing the propagated errors on mass-fractionation corrected Ca isotopic ratios.

The Ca isotopic composition of the double spike (excluding $^{46}Ca/^{40}Ca$) in Table 1 was determined using combined IsoProbe MC-ICPMS and TIMS measurements. We used HPS_{new} as a bracketing standard to correct measured IsoProbe $^{42}Ca/^{44}Ca$ and $^{43}Ca/^{44}Ca$ for mass bias. These are regarded as the true isotopic ratios of our DS because internally-normalized values for these ratios are accurate relative to TIMS. They are shown as I_{42} and I_{43} in Fig. 3. The high loading blank (20 ng from an old emitter compared with only 1ng with new emitter) compromised the TIMS measurements of DS, so TIMS data represent blank-DS mixtures, and offset from isotopic mixing lines by the instrumental mass fractionation. In a 3-isotope plot of $^{42}Ca/^{44}Ca$ vs. $^{43}Ca/^{44}Ca$, a mixing line is defined by the true unspiked natural sample (in this case the blank) and the true DS. We use the accepted natural Ca isotopic ratios from DePaolo (2004) as the true Ca isotopic ratios of the blank and the mass-bias corrected IsoProbe ratios as the true $^{42}Ca/^{44}Ca$ and $^{43}Ca/^{44}Ca$ of the DS (Fig. 3a). The intersection of the mixing line with the TIMS fractionation line gives the fractionation-corrected $^{42}Ca/^{44}Ca$ and $^{43}Ca/^{44}Ca$ for the blank-DS mixtures measured on TIMS (Fig. 3a). Once the normalized $^{42}Ca/^{44}Ca$ ratio of the blank-DS mixture was established by this procedure, normalized $^{40}Ca/^{44}Ca$ and $^{48}Ca/^{44}Ca$ ratios were calculated from the respective measured TIMS ratios (shown as T_{40} and T_{48} in Fig. 3b & 3c). Since the normalized $^{42}Ca/^{44}Ca$ of the spike is known from the IsoProbe data, mixing lines between the natural Ca and the normalized blank-DS mixture define the other true Ca isotopic ratios ($^{40}Ca/^{44}Ca$ and $^{48}Ca/^{44}Ca$, shown as I_{40} and I_{48} in Fig. 3b & 3c) in the double spike. Note that the isotopic ratios of our DS obtained from the above method (Fig. 3 & Table 1) are not absolute values because they are based on a standard (HPS_{new}) whose absolute $^{42}Ca/^{44}Ca$ ratio is unknown but assumed to be the DePaolo (2004) value. However, these values are close enough to the true ratios and will not affect the delta values.

For sample analysis, sample-DS mixtures were adjusted to have an optimum sample/ spike molar ratio close to 86:14 (Rudge et al., 2009). Measured Ca isotopic ratios of sample-spike mixtures were corrected off line for mass fractionation using a Matlab model

(Supplementary material C). This model resolves iteratively the true $^{40}Ca/^{44}Ca$, $^{48}Ca/^{44}Ca$, and $^{42}Ca/^{44}Ca$ ratios of the sample and mixture using the true spike isotopic ratios ($^{40}Ca/^{44}Ca$, $^{48}Ca/^{44}Ca$, and $^{42}Ca/^{44}Ca$), the measured $^{40}Ca/^{44}Ca$, $^{48}Ca/^{44}Ca$, and $^{42}Ca/^{44}Ca$ ratios of the mixture and the sample (we use values from DePaolo (2004) for the sample as first part of iteration). The correction model is based on two assumptions: 1) Ca mass fractionation follows exponential law and 2) the true isotopic ratio of the mixture should fall on the line defined by true DS and true sample isotopic ratios in a 3-isotope diagram. The detailed equations used in the model and the iteration are shown in Supplementary material C. The true isotopic ratios of minor isotopes ($^{43}Ca/^{44}Ca$ and $^{46}Ca/^{44}Ca$) of the sample and mixture can then be calculated using the same mass bias obtained from the true $^{40}Ca/^{44}Ca$ and measured $^{40}Ca/^{44}Ca$ ratios.

2.6 Ca isotopic analysis of natural apatite and aragonite by LA-MC-ICPMS

Additional tests on spatially-resolved Ca isotopic analysis (including ^{40}Ca) were also conducted directly in solid samples of Durango apatite and Tridacna aragonite thick sections (100 μm) using the GV IsoProbe MC-ICPMS coupled to an ArF (193nm) excimer LA system at RHUL (Muller et al., 2009). The IsoProbe MC-ICPMS allows direct measurements of ^{40}Ca because its hexapole collision cell with a small bleed of H_2 gas (0.8 ml/min) can eliminate the Ar-species interferences. Such *in-situ* Ca isotopic (including ^{40}Ca) analysis by LA-MC-ICPMS is used for direct comparison with corresponding TIMS data. Durango apatite and Tridacna aragonite were analysed with calcite SRM 915b pressed powder pellet as a bracketing standard. The operating conditions of the LA-MC-ICPMS and the cup configurations are provided in Supplementary material D.

3 Results and discussion

3.1 Internally-normalized Ca-isotopic ratios of unspiked samples

Standards SRM 915b, HPS_{new}, Fisher07, SRM 1486 (bone meal), and Durango apatite show no significant difference between them in their internally-normalized Ca isotopic ratios to $^{42}Ca/^{44}Ca$ of 0.31221 (DePaolo, 2004, Table 2 & Fig. 4). A total 64 measurements of the five standards obtained over 15 months result in average $^{40}Ca/^{44}Ca$ of 47.161 ± 0.011; $^{43}Ca/^{44}Ca$ of 0.064866 ± 0.000005, $^{46}Ca/^{44}Ca$ of 0.001515 ± 0.000006 and $^{48}Ca/^{44}Ca$ of 0.088687 ± 0.000037 (errors are 2SD). These data show uncertainties smaller than do the most recently published TIMS Ca isotopic data (Huang et al., 2012), and are consistent with the values of DePaolo (2004). Identical internally-normalized Ca isotopic ratios, achieved for

calcite, natural apatite and bioapatite without chemical separation (Fig. 4), suggest no need of chemical purification for TIMS Ca isotopic analysis on these materials. It should also be pointed out that these samples are 38 – 39 % Ca by weight, making it possible to skip the chemical separation step. For samples with lower Ca concentrations, however, chemical separation/purification is still necessary and will help to improve the precision of the measurements.

Ion exchange chromatography can efficiently remove ions from samples that can potentially cause interferences on Ca isotopes (e.g. $^{88}Sr^{2+}$ on ^{44}Ca). This approach is more critical for MC-ICPMS Ca isotopic analysis than TIMS because more interferences (such as hydrocarbons,oxides and doubly-charged ions) are present in the hot plasma (~ 6000 °C). For TIMS analysis, mass 43.5 (of $^{87}Sr^{2+}$) was monitored to check for doubly charged Sr interferences, although the much higher second ionization energy of Sr (compared with the low first ionization energy of Ca) would suggest this to be unlikely (Supplementary material B). As shown in Fig. 5, $^{88}Sr^{2+}$ interference on $^{44}Ca^{+}$ is negligible because measured raw TIMS $m43.5/m44$ ratios of Ca isotopic standards range between -6×10^{-6} to 6×10^{-6} and have no effect on the raw measured ratios of $m40/m44$. In contrast, the $m43.5/m44$ ($^{87}Sr^{2+}/^{44}Ca$) ratios, measured on both solution and laser mode by IsoProbe MC-ICPMS, are as high as 2×10^{-3} in Tridacna aragonite, Durango apatite, and Ca isotopic standards. This requires accurate correction. Alghough the IsoProbe MC-ICPMS allows measurements of ^{40}Ca – ^{46}Ca with Sr^{2+} interferences monitored at mass 43.5, it requires a magnetic field jump. It is also difficult to correct for ^{46}Ti interference on ^{46}Ca, as possible monitor isotopes have similar abundance to 46Ti, and cannot be accommodated with only two jumps in magnetic field (Supplementary material D & E). Because of partially resolved hydrocarbon interferences, the usable peak flats are quite narrow (0.01 – 0.02 amu, Supplementary material E), and thus the field jump may result in variation in the amount of interference that cannot be corrected. The difficulty of correcting for Ti interference means that it must be removed by ion exchange chemistry before analysis.

3.2 Double spike corrected $\delta^{44/40}Ca$

All measured Ca isotopic ratios of standards and samples were corrected using the DS Matlab model (Supplementary material C). The 16 spiked primary standard SRM 915b measurements (Table 3) give an average DS-corrected ratio of 47.236 ± 0.011 for $^{40}Ca/^{44}Ca$, 0.312477 ± 0.000036 for $^{42}Ca/^{44}Ca$, and 0.088585 ± 0.000019 for $^{48}Ca/^{44}Ca$ (all errors are

2SD). These values are different from the internally-normalized Ca isotopic ratios of the unspiked SRM 915b (Table 2 & Fig. 4), but they are used for the calculation of δ-values of secondary standards and samples. Because our primary standard (SRM 915b), secondary standards and samples were corrected in the exactly the same way, the delta values are absolute and independent of both DS and SRM 915b Ca isotopic composition used to calculate them. The delta notation is expressed as $\delta^{44/40}Ca$ relative to SRM 915a, using the conversion equation $\delta^{44/40}Ca^{sample}_{SRM\ 915a} = \delta^{44/40}Ca^{sample}_{SRM\ 915b} + \delta^{44/40}Ca^{SRM915b}_{SRM\ 915a}$. The value of $\delta^{44/40}Ca^{SRM915b}_{SRM\ 915a}$ is 0.72 ‰, determined by Heuser & Eisenhauer (2008).

The average DS-corrected $\delta^{44/40}Ca$ values of HPS_{new}, Fisher 07, Durango apatite and SRM 1486 (bone meal) are shown in Table 3 and plotted in Fig 5. HPS_{new} and Fisher07 show average $\delta^{44/40}Ca$ values of 0.70 ± 0.18 ‰ (2SD, n = 12) and 1.03 ± 0.20 ‰ (2SD, n = 11), respectively. Durango apatite solutions made from both laser-cut (A1, A2, B1, B2 and C) and the non-laser cut pieces yield an average $\delta^{44/40}Ca$ (0.70 ± 0.17 ‰, 2SD, n = 15) identical to that of HPS_{new}. The average $\delta^{44/40}Ca$ value of SRM 1486 (bone meal) is -1.03 ± 0.19 ‰ (2SD, n = 9). The delta values of Ca isotopic standards HPS_{new}, Fisher 07 and bone meal in Fig. 6 fall well within published data ranges and averages (Heuser and Eisenhauer, 2008; Reynard et al., 2010; Heuser et al., 2011; Tacail et al., 2014), validating our analytical method and DS-correction technique. Our external reproducibility of ~ 0.20 ‰ (2SD) on $\delta^{44/40}Ca$ values is similar to that achieved on HPS_{new} and Fisher07 using MC-ICPMS (Reynard et al., 2010), and on SRM 1486 (bone meal) using both TIMS and MC-ICPMS (Heuser and Eisenhauer, 2008; Heuser et al., 2011; Tacail et al., 2014).

3.3 $\delta^{44/40}Ca$ of Durango apatite

3.3.1 TIMS analyses

Eight TIMS analyses of Durango apatite solution made of non-laser cut pieces give an average $\delta^{44/40}Ca$ of 0.70 ± 0.21 ‰ (2SD). The $\delta^{44/40}Ca$ values of laser-cut Durango apatite fragments (A1, A2, B1, B2 and C) vary slightly from 0.60 ± 0.06 ‰ (2SE) to 0.80 ± 0.10 ‰ (2SE). The two pieces with large laser-induced surface damage (A1 and A2) show similar values within the error to the other 3 fragments without any surface laser damage (Fig. 6). The large error bars on fragment B2 (and B2_re) are simply a consequence of short analysis of a small Ca loading (~1μg). Overall, the five fragments give an average $\delta^{44/40}Ca$ of 0.70 ± 0.13 (2SD), in excellent agreement with that of the non-laser cut Durango apatite solution.

This suggests negligible laser-induced mass fractionation on Ca isotopes in apatite using our laser-cutting method. This is not too surprising considering the small laser-effected areas (edges and shallow surface) being only 1/50 of the large volume of the sample fragments. Also, such effects are not expected and have not been demonstrated before.

3.3.2 For precise micro-sampling, our laser-cutting method offers more advantages over micromilling (Charlier et al., 2006). Similar laser microsampling approach has also been applied to achieve spatial control for in-situ Rb-Sr dating of mineral phases in fine-grained rocks (Egli et al., 2015). The wet-micromilling in a water drop presented by Charlier et al. (2006) produces powder samples that can more easily be contaminated by Ca from the background during handling and are difficult to clean. On the other hand, the automated laser-cutting process is faster and minimizes material loss; and laser-cut fragments are easier to handle, clean and maintain low handling errors. Additionally, for cutting intricate shapes such as growth lines particularly in small bio-apatite (e.g. enamel cuboids), the laser beam allows more controlled cutting of complex shapes of almost any size, (e.g. isochronally cutting along the Retzius lines), a great improvement over previous micromilling.LA-MC-ICPMS analysis

The measured ratios ($^{42}Ca/^{44}Ca$, $^{43}Ca/^{44}Ca$ and $^{40}Ca/^{44}Ca$) of Tridacna aragonite and Durango apatite after Sr correction for a single day analysis by LA-MC-ICPMS are presented together with the bracketing standard SRM 915b pellet in Fig. 7. Tridacna aragonite and Durango apatite clearly show higher measured ratios than SRM 915b. The three materials do not show consistent measured ratios during the one-day course of analysis.

The measured ratios $^{40}Ca/^{44}Ca$ and $^{42}Ca/^{44}Ca$ of Tridacna aragonite decreased after the introduction of standard SRM 915b with lower measured Ca ratios (Fig. 7). Measured $^{43}Ca/^{44}Ca$ ratios do not show any obvious change because ^{43}Ca is such a minor isotope resulting in large relative ratio uncertainties. Similar effects, although to a less degree, can also be seen in the measured Durango apatite ratios for the same reason (e.g. matrix mismatch between calcite and apatite). This effect can not be a memory issue because gas blanks between samples have overall consistent $^{40}Ca/^{44}Ca$ ratios and have ^{40}Ca intensity 4000 times less than that of the sample. It is also not caused by Sr^{2+} or other interferences because these ratios have been already corrected for Sr interference and the internally-normalized Ca

isotopic ratios over one day of analysis are constant (Supplementary material E). Hence, our LA results indicate that the change of matrix between aragonite and calcite and between calcite and apatite has caused changes in instrumental sensitivity and mass bias. Matrix match is therefore a must for laser ablation analysis.

The average $\delta^{44/40}$Ca of Durango apatite corrected using the standard-sample bracketing technique is -1.82 ± 0.46 ‰ (2SD, n = 4), relative to SRM 915a. This value is very different from the average value (0.70 ± 0.17 ‰, 2SD, n = 15) of the same Durango apatite obtained from TIMS analysis. The large discrepancy between our TIMS and LA-MC-ICPMS data of the same Durango apatite is mainly due to the inaccuracy of the latter, possibly caused by matrix effects. However, TIMS analysis of Durango apatite (including laser-cut and non-laser cut pieces, see Fig. 6) has demonstrated its homogeneity in Ca isotopes, so it might have a potential to become an in-house apatite standard for LA-MC-ICPMS analysis on Ca isotopes.

Other workers have also attempted to measure in-situ Ca isotope variations ($\delta^{44/42}$Ca and $\delta^{43/42}$Ca) in tooth enamel by High Resolution (HR)-LA-MC-ICPMS, using sintered SRM 1400 (bone ash) and sintered powder synthetic apatite (doped or not with Sr) as LA standards for close matrix match (Tacail et al., 2015). Despite careful tuning of instrumentation and extensive correction for Sr interferences, the external reproducibility (2SD) on $\delta^{44/42}$Ca is between 0.51 ‰ to 1.16 ‰ for 4 and 200 measurements (Tacail et al., 2015). This is equivalent to 1.02 – 2.32 ‰ (2SD) on $\delta^{44/40}$Ca, and hence the delta values areunable to reflect any intra-enamel variations at this scale. In-situ Ca isotope analysis by LA- MC-ICPMS, although fast and the least destructive to precious samples, is still far away from reaching the precision and accuracy already achieved by TIMS and MC-ICPMS.

3.4 TIMS $\delta^{44/40}$Ca profile of a modern human third molar

Ca isotopic data of microsamples extracted from the enamel of a modern human third molar are shown in Table 4 and Fig. 8. The values of $\delta^{44/40}$Ca vary from -0.71 ± 0.03 ‰ to 0.03 ± 0.05 ‰ (2SE). The 0.74 ‰ range is three times larger than the external reproducibility (0.20 ‰), and thus considered significant. The $\delta^{44/40}$Ca value initially increases from -0.55 ‰ to -0.02 ‰ at age ~ 11.5 before it drops to -0.71 ‰ at age ~ 12. It then rises to around -0.15 ‰ just after age ~ 12.5 and remains essentially invariant until age ~ 14. The age estimates are explained below.

The analysed wisdom tooth is the lower left third molar (tooth code: 38) of a female individual from Central China. On the basis of radiographs, the development and mineralization of third molars in Chinese females (Han people) begin at the age of 11 ± 1, while crown formation (including enamel and dentine) is completed at the age 14 ± 1 (Bai et al., 2008; Zeng et al., 2010); these ages overall are in line with the comprehensive human tooth development atlas developed recently by AlQahtani et al. (2010). This female lived a stable life with a balanced diet in a medium-sized city near Central China during childhood and adolescence (age 0 – 17), so should be consistent with the above statistics. Due to the slight incompleteness at the bottom of the right-side enamel (Fig. 8), we assume that the above $\delta^{44/40}$Ca profile is likely to represent a time period between the age of 11 and 14. When taking into account the size of each microsample (180 × 500 μm), we assign a very approximate interval of ~ 6 months to each of the right enamel microsamples (1R to 6R), and ~ 3 – 4 months to each of the 9 left microsamples (1L to 9L). It should be pointed out that tooth enamel grows non-linearly with more time presented towards the roots, the above age estimations are only approximate between the two known end members of age (11 & 14 yrs). Also, microsamples 3R and 3L were not plotted in Fig. 8 because the former was lost during sample preparation and the latter and its repeat (3L_Re) have very small sample weight so are very short runs with large errors (Table 2).

Tooth mineralization can reflect the physiological state of humans (e.g. birth, weaning, puberty, diseases, FitzGerald et al., 2006). The third molars mineralize during the adolescence and therefore ideally reflect physiological changes in puberty. Girls on average begin puberty at ages ~11, followed by a pubertal growth sprout for 3 years, and complete physical maturity by age ~15 – 16 (Theintz et al., 1992; Kail and Cavanaugh, 2010). Puberty has a fundamental role in bone mass growth. The need of Ca is greatly increased in puberty (Saggese et al., 2002). Dietary Ca absorption and Ca retention are found to peak during early puberty (11 - 12yrs) and then reduced in late puberty (Abrams and Stuff, 1994). Bone turnover (including both bone formation and resorption), reflected by biomarkers, also reaches maximum during accelerated pubertal growth (Blumsohn et al., 1994). Maximal bone mass accretion is found to occur later in puberty (Cadogan et al., 1998; Saggese et al., 2002). Menarche is a single event in the combination of girls' physical changes during puberty, and its associated female hormone oestrogen has shown to facilitate bone accretion in early puberty (Boot et al., 1997; Cadogan et al., 1998).

Skulan and DePaolo (1999) first presented a Ca isotope transport model for vertebrates that illustrates Ca isotope fractionation along Ca pathways. According to this simple model, Ca isotope fractionation only takes place during bone mineralization, with a bone-diet difference ($\Delta_{bone\text{-}diet}$) in $\delta^{44/40}Ca$ of -1.3 ‰. However, Skulan et al. (2007) and Heuser & Eisenhauer (2010) found that isotope fractionation also occurs between soft tissue and excreted Ca in urine due to physiological processes in kidneys. Here, a combined Ca isotope transport model in mammals (Fig. 9) is present here, that is based on the orignal model of Skulan and DePaolo (1999), but with the later discovery on Ca isotope fractionation in excretions (Heuser et al., 2007; Skulan et al., 2007; Heuser and Eisenhauer, 2010), and the addition of tooth formation, to show an up-to-date understanding of Ca isotope fractionation during metabolism in mammals.

Skulan and DePaolo (1999) suggested that Ca isotopic values of soft tissue and bone depend on dietary calcium use efficiency and bone mineral balance. During effective bone growth when large amount of dietary Ca is absorbed and fixed in bones, both bone and soft tissue will have much higher $\delta^{44/40}Ca$; and when bone loss is dominant, the isotopic composition of bone and soft tissue will be lighter. So, effective bone growth leads to a decrease of bone - diet offset ($\Delta_{bone\text{-}diet}$) whereas net bone loss does the opposite. Taking a percent net Ca absorption of Ca of 30 – 36% during adolescence (Matkovic, 1991; Abrams and Stuff, 1994), model predicted bone $\delta^{44/40}Ca$ increase due to fast skeletal growth could be 0.4 – 0.5 ‰ when diet $\delta^{44/40}Ca$ is fixed (Skulan and DePaolo, 1999; Reynard et al., 2013). For the analysed young Chinese female, if the dietary $\delta^{44/40}Ca$ is mostly invariant in her pubertal period, bone $\delta^{44/40}Ca$ should theoretically show an increasing trend in $\delta^{44/40}Ca$ from early to late puberty. However, dietary change (e.g. milk-consumption) can easily cancel the growth contribution in bone $\delta^{44/40}Ca$ because milk and dairy products have distinctly low $\delta^{44/40}Ca$ (Chu et al., 2006).

No studies have demonstrated the relationship among tooth, bone, diet and soft tissue $\delta^{44/40}Ca$ ratios. The third molar calcification is poorly correlated with skeletal maturity and pubertal growth (Garn et al., 1962; Thompson et al., 1975; Krailassiri et al., 2002; Uysal et al., 2004), despite the racial variations in the relationship predominantly caused by ethnic origin, climate, nutrition, urbanization and so on (Mappes et al., 1992). Only one study reported a statistically-strong correlation between lower third molar development, skeletal maturity and chronological age (Engström et al., 1983); however, their differentiation of third molar

developmental stage is too broad compared with the well-acknowledged eight stage of tooth calcification by Demirjian et al. (1973); and within each tooth calcification stage, variations in age and skeletal stage are too large to show the strong correlation convincingly. This is not surprising considering the different biomineralization mechanisms of enamel, dentin and bone. Enamel mineralization is controlled by ameloblasts, cells that secret calcium and phosphate from blood to form and then harden enamel crystals (Smith, 1998). However, the formation of dentin and bone is controlled by odontoblast (cell that deposit dentin) and osteoblast, cells that synthesizes matrix and arrange bone formation and remodelling (Boskey, 2007). This biological difference between enamel and dentin is also shown by a $\Delta_{dentin\text{-}enamel}$ of 0.3 – 0.4 (Heuser et al., 2011). Enamel-bone offset in calcium isotope composition is probably on a similar scale as bone and dentin are quite similar in mineral and organic contents.

The crown formation (enamel + dentin) of this third molar covers the periods of early puberty and the pubertal growth spurt, but doesn't necessarily show accelerated growth pattern like bones for reasons mentioned above. While over 90% of the absorbed dietary Ca is used for building bones, a small portion of the dietary Ca is still used in tooth mineralization in adolescence. Calcium ions can be removed rapidly from blood stream into ameloblasts (ruffle-ended), possibly via Ca-blinding proteins, or passive ion exchange with Na^+ through membrane, or active pumping with metabolic cost (Smith, 1998). At the start of the enamel formation (the onset of the puberty) when net bone growth is still small, soft tissue and diet should have very similar Ca isotope ratios and the bone-diet offset ($\Delta_{bone\text{-}diet}$) very close to the steady state value (-1.3 – -1.5 ‰, Skulan and DePaolo, 1999; Reynard et al. 2013). Bone and enamel have the same source Ca (intestinal Ca absorbed from diet); and enamel has a calcium isotope composition different by the enamel-diet offset ($\Delta_{enamel\text{-}diet}$). The main factor in this period that can change enamel $\delta^{44/40}Ca$ is likely to be its source – the diet. This female had a diet with dairy product intake (mainly formula milk) in her childhood, then changed in the beginning of her adolescence to a dairy-free, but otherwise balanced diet. According to Chu et al., (2006), a dairy rich, health diet containing all major food sources (vegetable/fruits, grains/cereal, meat and water) is 0.63 ‰ lighter than a dairy-free diet with balanced nutrition. Assuming a constant diet-enamel Ca isotope fractionation in humans, the above two diets would yield the same difference of 0.63 ‰ in enamel $\delta^{44/40}Ca$. These observed increase of 0.53 ‰ in $\delta^{44/40}Ca$ is more likely the result of dairy-rich to dairy-free diet switch, rather than bone growth in this period

The drop of $\delta^{44/40}$Ca probably occurred at the age of 12 (Fig. 8), which coincides with this female's menarcheal age. During this early stage of pubertal growth, when bone turnover and bone remodelling was fast, net bone formation should be more than the start of puberty, but less than the late puberty stage when bone mineral density was the highest. Bone and soft tissue probably had higher $\delta^{44/40}$Ca at this time than the onset of puberty. Ca isotope pool for third molar mineralization was likely to be regularly supplied with blood Ca, but ameloblast cells actively gate Ca ions selectively for very short period of time (seconds or milliseconds) repeatedly during enamel maturation. If there was no Ca isotope fractionation through active selection of Ca by amloblasts, the Ca isotope composition of enamel should be similar to the blood $\delta^{44/40}$Ca at the same time scale (over several hours, Skulan and DePaolo, 1999), and should show a slight increase in $\delta^{44/40}$Ca as more and more light Ca isotopes are secreted in the bones. However, tooth enamel showed a drop of $\delta^{44/40}$Ca by 0.73 ‰. This peculiarity may be related to the biologically controlled Ca movement by amloblasts. It might also be a result of physiological change – menarche and the effects of its associated female hormones (e.g. estrogen), or the complexity of the interaction between female hormones and tooth formation proteins.

Based on data from just one individual, we cannot assume that this phenomenon is general. More $\delta^{44/40}$Ca data from third molars of both females and males are clearly needed to address this issue. Such a population study is beyond the scope of this paper. And finally, slightly higher, but essentially invariant $\delta^{44/40}$Ca between ages ~12.5 and 14 may suggest that the individual was eating a consistent mixed diet, and that her body was in a steady fast growing status with effective bone formation through mid-adolescence.

On the other hand, using the diet-bone isotope fractionation of 1.3 ‰ in $\delta^{44/40}$Ca (Chu et al., 2006), the dairy-rich and dairy-free diets would result in bone $\delta^{44/40}$Ca of –2.34 ‰ and –1.71 ‰, respectively. Tooth enamel $\delta^{44/40}$Ca may be even more negative than bone $\delta^{44/40}$Ca (Heuser et al., 2011). Two Ca isotope analyses of European female third molars by solution MC-ICPMS give a range of -1.81 – 2.08 ‰ (with 2SD varying from ± 0.2 to ± 1.27 ‰, Tacail et al., 2015). However, these values are more negative than the average $\delta^{44/40}$Ca of -0.22 ‰ observed for this Chinese young female. This may indicate geographical variations in Ca isotopic ratios of food sources, caused by source bedrock, sediments and water with different calcium isotopic composition in different regions. However, there are very limited Ca isotopic data of different food sources in China.

In this individual case, the $\delta^{44/40}$Ca profile of tooth enamel can reveal information about an individual's dietary structure, and more perhaps physiological effects on Ca isotope fractionation when knowing the individual's life history. It may help identifying the time periods of minimal physiological influence (e.g. age ~12.5 – 14 in Fig. 8) for reliable interpretation of the environmental signals from $\delta^{44/40}$Ca profiles in fossil human teeth.

4 Conclusions

(1) Our newly-developed laser microsampling technique provides solid fragments (rather than powder) at the scale of tens of micrometres that facilitate easy cleaning and maintain low Ca contamination. It offers minimum material loss, great flexibility, and can constrain well sampling along the isochronous growth lines in biogenic phosphate or calcite samples (e.g. Retzius lines in tooth enamel).

(2) No ion exchange chromatography is required for accurate and precise Ca isotopic analysis by TIMS on natural calcite and apatite because these materials without chemical purification show identical internally-normalized $^{40}Ca/^{44}Ca$ and $^{48}Ca/^{44}Ca$ ratios (to $^{42}Ca/^{44}Ca$ of 0.31221), consistent with the values of DePaolo (2004).

(3) Parafilm dam loading can confine the sample spread to ~1 mm on a Re-filament and achieve an in-run fractionation on Ca of as low as 0.7 ‰, which reduces the chances of mixing between different Ca reservoirs on a single Re-filament.

(4) The average ^{42}Ca–^{48}Ca double spike corrected $\delta^{44/40}$Ca of 0.70 ± 0.18 ‰ (2SD) for HPS_{new}, 1.03 ± 0.20 ‰ (2SD) for Fisher07 and -1.03 ± 0.19 ‰ (2SD) for SRM 1486 (bone meal), relative to SRM 915a, agree well with the published data for these standards.

(5) Identical TIMS $\delta^{44/40}$Ca values were obtained on Durango apatite solutions made from both laser-cut and non-laser cut fragments. This result indicates no detectable laser-induced mass fractionation on Ca isotopes in such materials.

(6) The $\delta^{44/40}$Ca profile of a modern human's third molar reflects a pattern that doesn't follow the relationship and box model of Skulan & Depaolo (1999) expected between diet, soft tissue and bone in their calcium isotopic composition during bone formation. However, it shows dietary effects and connection between key physiological change and Ca isotope excursion. A comprehensive understanding of physiological effects on

Ca isotope fractionation in modern fauna will help to extract reliable environmental records from $\delta^{44/40}$Ca profiles in fossil teeth.

(7) Poor accuracy of IsoProbe MC-ICPMS analysis for Ca isotope ratios is caused by the following issues: a) The magnetic field jump, coupled with narrow interference-free peak flats, means that it is difficult to ensure a constant magnitude of hydrocarbon interference that can be corrected by on-peak zero subtraction; b) Ti interference (if not removed during chemistry) means that double spike mass fractionation corrections using ^{46}Ca or ^{48}Ca are untenable. Further, in-situ direct Ca isotope analysis of natural calcite, aragonite and apatite by LA-MC-ICPMS shows strong matrix sensitivity, and therefore requires close matrix match.

Acknowledgements

We are indebted to Linda Reynard for discussions on Ca isotope methodology early on. We thank Andy Carter for supplying Durango apatite, and Carrie Wright for Ca isotopic standard solutions. Viola Warter is thanked for helping with the use of the laser-ablation system at RHUL. This work was funded via Leverhulme Trust Research Project Grant RPG-156, which is gratefully acknowledged.

588 **List of Figures**

589 Fig. 1 Laser-cutting strategy of a thick-section from a modern human wisdom tooth (CLW2).
590 Two long laser tracks (blue lines) were placed along the enamel-dentine junction (EDJ, white
591 line) with an offset of 180 μm, and short laser tracks (blue lines) across these two lines at an
592 interval of 500 μm. Rectangular microsamples (180 × 500 μm) were retrieved from this
593 section: namely 1R – 6R from the right part and 1L – 9L from the left part. Unfortunately,
594 several of the left-side microsamples were broken and lost during cleaning and weighing as
595 the pieces were only a few micrograms and hardly visible under the naked eye.

596 Fig. 2 A Durango apatite thick section (100 μm) showing 5 laser-cut fragments (A1, A2, B1,
597 B2 & C). Note that fragments A1 and A2 have additional laser tracks on the surface.

598 Fig. 3 Cross-diagrams demonstrating the normalization of double spike (DS) Ca isotopic
599 composition using both IsoProbe and TIMS Ca isotope data. The corrected DS isotopic ratios
600 (I_{40}, I_{42}, I_{43} and I_{48}), also called the true DS isotopic composition ($^{40}Ca/^{44}Ca_{corrected\text{-}IsoProbe}$,
601 $^{42}Ca/^{44}Ca_{IsoProbe}$, $^{43}Ca/^{44}Ca_{IsoProbe}$ and $^{48}Ca/^{44}Ca_{corrected\text{-}IsoProbe}$) are also listed in Table 1.

602 Fig. 4 Internally-normalized TIMS $^{40}Ca/^{44}Ca$, $^{43}Ca/^{44}Ca$ and $^{48}Ca/^{44}Ca$ ratios (to $^{42}Ca/^{44}Ca$ =
603 0.31221, DePaolo, 2004)) versus the measured $^{40}Ca/^{44}Ca$ ratios of 4 standards (SRM 915b,
604 HPS_{new}, Fisher07, SRM 1486 bone meal) and Durango apatite obtained over 15 months. The
605 average normalized-ratios and 2SD are plotted as grey solid and dashed lines. Note that there
606 is no obvious difference in normalized ratios between the analysed materials (calcite and
607 apatite).

608 Fig. 5 Measured raw ratios of *m*43.5/*m*44 on TIMS and LA-MC-ICPMS. The individual error
609 bars (2SE) on TIMS *m*43.5/*m*44 are not plotted because they are almost as large as half of the
610 data range, so only an indicative key is shown here at the right bottom.

611 Fig. 6 Double-spike corrected $\delta^{44/40}Ca$ ratios of Ca isotopic standards (HPS_{new}, Fisher07 and
612 SRM 1486 bone meal) and Durango apatite shown relative to published delta values. The
613 individual error bars plotted are 2SE. Durango apatite plot includes data of laser-cut (A1, A2,
614 B1, B2 and C) and the non-laser cut pieces. The average (black solid line) and the 2SD (grey
615 dashed lines) are also plotted. Our SRM 1468 (bone meal) data yield the identical average
616 $\delta^{44/40}Ca$ value (black solid line) to that in Heuser & Eisenhauer (2008), shown as a purple
617 line. The dashed lines show 2SD.

Fig. 7 Measured Ca isotopic ratios of SRM 915b pellet, Tridacna aragonite and Durango apatite obtained in one day by LA-MC-ICPMS, with 34 μm laser tracks, a scan speed of 1 mm/min and laser repetition rate of 5Hz. Data are corrected for Sr interference, but not for mass fractionation.

Fig. 8 $\delta^{44/40}$Ca profile of a lower left third molar from a contemporaneous Chinese female, error plotted are 2SE. Reproducibility (2SD) is shown as an indicative key. Laser-cut microsamples (blue rectangles) were retrieved from both left (L) and right (R) side of the enamel. Microsamples 4R and 5R each have a repeat, named as 4R_Re and 5R_Re.

Fig. 9 Ca isotope transfer model in mammals showing Ca isotope fractionations along the paths and the relationships in $\delta^{44/40}$Ca between diet, soft tissue, bones/teeth and excretions. It is modified from Skulan & DePaolo (1999) and Heuser & Eisenhauer (2010). Note that the relationship between diet and feces Ca isotope ratios ($\delta^{44/40}Ca_f \approx \delta^{44/40}Ca_d$) is based on the mini-pigs study by Heuser et al. (2007), the enamel-dentine offset ($\Delta_{enamel\text{-}dentin}$) is from Heuser et al. (2011), and the reference for root resorption of deciduous teeth is Harokopakis-Hajishengallis (2007).

633 **List of Tables**

634 Table 1. Ca isotopic ratios and abundance of ^{42}Ca–^{48}Ca double spike (DS) solution. Note that
635 the isotopic abundances were calculated from the weights of each spike in the DS solution
636 and their certified values of abundance.

637 Table 2. TIMS Ca isotopic ratios of standards SRM 915b, HPS_{new}, Fisher07, SRM 1486
638 (bone meal), and Durango apatite, internally-normalized to $^{42}Ca/^{44}Ca$ of 0.31221 (DePaolo,
639 2004).

640 Table 3. The mean DS-corrected TIMS Ca isotopic ratios and $\delta^{44/40}Ca$ of the Ca isotopic
641 standards, relative to 915a.

642 Table 4. TIMS Ca isotopic data of the laser-cut microsamples extracted from a lower left
643 third molar of a young Chinese female (CLW2). $^{40}Ca/^{44}Ca_T$, $^{48}Ca/^{44}Ca_T$ and $^{42}Ca/^{44}Ca_T$ are
644 double spike (DS) corrected ratios.

645

Reference:

Abrams, S.A., Stuff, J.E., 1994. Calcium metabolism in girls: current dietary intakes lead to low rates of calcium absorption and retention during puberty. The American journal of clinical nutrition 60, 739-743.

AlQahtani, S.J., Hector, M., Liversidge, H., 2010. Brief communication: the London atlas of human tooth development and eruption. American journal of physical anthropology 142, 481-490.

Bai, Y.M., Mao, J., Zhu, S.R., Wei, W., 2008. Third-Molar Development in Relation to Chronologic Age in Young Adults of Central China. Journal of Huazhong University of Science and Technology-Medical Sciences 28, 487-490.

Blumsohn, A., Hannon, R., Wrate, R., Barton, J., AI□Dehaimi, A., Colwell, A., Eastell, R., 1994. Biochemical markers of bone turnover in girls during puberty. Clinical Endocrinology 40, 663-670.

Boot, A.M., de Ridder, M.A., Pols, H.A., Krenning, E.P., de Muinck Keizer-Schrama, S.M., 1997. Bone Mineral Density in Children and Adolescents: Relation to Puberty, Calcium Intake, and Physical Activity 1. The Journal of Clinical Endocrinology & Metabolism 82, 57-62.

Boskey, A.L., 2007. Mineralization of bones and teeth. Elements 3, 385-391.

Brazier, J.-M., Suan, G., Tacail, T., Simon, L., Martin, J.E., Mattioli, E., Balter, V., 2015. Calcium isotope evidence for dramatic increase of continental weathering during the Toarcian oceanic anoxic event (Early Jurassic). Earth and Planetary Science Letters 411, 164-176.

Cadogan, J., Blumsohn, A., Barker, M.E., Eastell, R., 1998. A longitudinal study of bone gain in pubertal girls: anthropometric and biochemical correlates. Journal of Bone and Mineral Research 13, 1602-1612.

Charlier, B., Ginibre, C., Morgan, D., Nowell, G., Pearson, D., Davidson, J., Ottley, C., 2006. Methods for the microsampling and high-precision analysis of strontium and rubidium isotopes at single crystal scale for petrological and geochronological applications. Chemical Geology 232, 114-133.

Chu, N.C., Henderson, G.M., Belshaw, N.S., Hedges, R.E.M., 2006. Establishing the potential of Ca isotopes as proxy for consumption of dairy products. Applied Geochemistry 21, 1656-1667.

Clementz, M.T., Holden, P., Koch, P.L., 2003. Are calcium isotopes a reliable monitor of trophic level in marine settings? International Journal of Osteoarchaeology 13, 29-36.

Demirjian, A., Goldstein, H., Tanner, J., 1973. A new system of dental age assessment. Human biology, 211-227.

DePaolo, D.J., 2004. Calcium isotopic variations produced by biological, kinetic, radiogenic and nucleosynthetic processes. Geochemistry of Non-Traditional Stable Isotopes 55, 255-288.

Egli, D., Müller, W., Mancktelow, N., 2015. Laser□cut Rb□Sr microsampling dating of deformational events in the Mont Blanc□Aiguilles Rouges region (European Alps). Terra Nova.

Engström, C., Engström, H., Sören, S., 1983. Lower third molar development in relation to skeletal maturity and chronological age. The Angle Orthodontist 53, 97-106.

Farkas, J., Buhl, D., Blenkinsop, J., Veizer, J., 2007. Evolution of the oceanic calcium cycle during the late Mesozoic: Evidence from $\delta^{44/40}$Ca of marine skeletal carbonates. Earth and Planetary Science Letters 253, 96-111.

692 Fietzke, J., Eisenhauer, A., Gussone, N., Bock, B., Liebetrau, V., Nagler, T.F., Spero, H.J.,
693 Bijma, J., Dullo, C., 2004. Direct measurement of $^{44}Ca/^{40}Ca$ ratios by MC-ICP-MS using
694 the cool plasma technique. Chemical Geology 206, 11-20.
695 FitzGerald, C., Saunders, S., Bondioli, L., Macchiarelli, R., 2006. Health of infants in an
696 Imperial Roman skeletal sample: perspective from dental microstructure. American
697 journal of physical anthropology 130, 179-189.
698 Garn, S.M., Lewis, A.B., Bonné, B., 1962. Third molar formation and its development course.
699 The Angle Orthodontist 32, 270-279.
700 Gussone, N., Eisenhauer, A., Tiedemann, R., Haug, G.H., Heuser, A., Bock, B., Nagler, T.F.,
701 Muller, A., 2004. Reconstruction of Caribbean sea surface temperature and salinity
702 fluctuations in response to the pliocene closure of the Central American Gateway and
703 radiative forcing, using $\delta^{44/40}Ca$, $\delta^{18}O$ and Mg/Ca ratios. Earth and Planetary Science
704 Letters 227, 201-214.
705 Halicz, L., Galy, A., Beshaw, N., O'Nions, R., 1999. High precision measurements of
706 calcium isotopoes in carbonates and related materials by multiple collector inductively
707 coupled plasma mass spectrometry (MC-ICP-MS). Journal of Analytical Atomic
708 Spectrometry 14, 1835-1838.
709 Harokopakis-Hajishengallis, E., 2007. Physiologic root resorption in primary teeth: molecular
710 and histological events. Journal of oral science 49, 1-12.
711 Hart, S.R., Zindler, A., 1989. Isotope fractionation laws: a test using calcium. International
712 Journal of Mass Spectrometry and Ion Processes 89, 287-301.
713 Heuser, A., Eisenhauer, A., 2008. The calcium isotope composition (delta Ca-44/40) of NIST
714 SRM 915b and NIST SRM 1486. Geostandards and Geoanalytical Research 32, 311-315.
715 Heuser, A., Eisenhauer, A., 2010. A pilot study on the use of natural calcium isotope (44
716 Ca/40 Ca) fractionation in urine as a proxy for the human body calcium balance. Bone 46,
717 889-896.
718 Heuser, A., Eisenhauer, A., Bohm, F., Wallmann, K., Gussone, N., Pearson, P.N., Nagler,
719 T.F., Dullo, W.C., 2005. Calcium isotope ($\delta^{44/40}Ca$) variations of Neogene planktonic
720 foraminifera. Paleoceanography 20.
721 Heuser, A., Eisenhauer, A., Gussone, N., Bock, B., Hansen, B.T., Nagler, T.F., 2002.
722 Measurement of calcium isotopes ($\delta^{44/40}Ca$) using a multicollector TIMS technique.
723 International Journal of Mass Spectrometry 220, 385-397.
724 Heuser, A., Eisenhauer, A., Scholz-Ahrens, K., Schrezenmeir, J., 2007. Biological
725 fractionation of Ca isotopes (δ 44/40 Ca): a study in Göttingen minipigs. Geochim
726 Cosmochim Acta 71, A402.
727 Heuser, A., Tutken, T., Gussone, N., Galer, S.J.G., 2011. Calcium isotopes in fossil bones
728 and teeth - Diagenetic versus biogenic origin. Geochimica Et Cosmochimica Acta 75,
729 3419-3433.
730 Hippler, D., Eisenhauer, A., Nagler, T.F., 2006. Tropical Atlantic SST history inferred from
731 Ca isotope thermometry over the last 140ka. Geochimica Et Cosmochimica Acta 70, 90-
732 100.
733 Hirata, T., Tanoshima, M., Suga, A., Tanaka, Y.K., Nagata, Y., Shinohara, A., Chiba, M.,
734 2008. Isotopic Analysis of Calcium in Blood Plasma and Bone from Mouse Samples by
735 Multiple Collector-ICP-Mass Spectrometry. Analytical Sciences 24, 1501-1507.
736 Holmden, C., Bélanger, N., 2010. Ca isotope cycling in a forested ecosystem. Geochimica Et
737 Cosmochimica Acta 74, 995-1015.
738 Huang, S.C., Farkas, J., Yu, G., Petaev, M.I., Jacobsen, S.B., 2012. Calcium isotopic ratios
739 and rare earth element abundances in refractory inclusions from the Allende CV3
740 chondrite. Geochimica Et Cosmochimica Acta 77, 252-265.

741 Kail, R., Cavanaugh, J., 2010. The Study of Human Development. Human Development: A
742 Life-span View (5th ed.). Belmont, CA: Wadsworth Cengage Learning.
743 Krailassiri, S., Anuwongnukroh, N., Dechkunakorn, S., 2002. Relationships between dental
744 calcification stages and skeletal maturity indicators in Thai individuals. The Angle
745 Orthodontist 72, 155-166.
746 Lehn, G., Jacobson, A., Holmden, C., 2013. Precise analysis of Ca isotope ratios ($\delta^{44/40}$Ca)
747 using an optimized ^{43}Ca–^{42}Ca double-spike MC-TIMS method. International Journal of
748 Mass Spectrometry 351, 69-75.
749 Lehn, G.O., Jacobson, A.D., 2015. Optimization of a ^{48}Ca–^{43}Ca double-spike MC-TIMS
750 method for measuring Ca isotope ratios ($\delta^{44/40}$Ca and $\delta^{44/42}$Ca): limitations from filament
751 reservoir mixing. Journal of Analytical Atomic Spectrometry.
752 Mappes, M.S., Harris, E.F., Behrents, R.G., 1992. An example of regional variation in the
753 tempos of tooth mineralization and hand-wrist ossification. American Journal of
754 Orthodontics and Dentofacial Orthopedics 101, 145-151.
755 Matkovic, V., 1991. Calcium metabolism and calcium requirements during skeletal modeling
756 and consolidation of bone mass. The American journal of clinical nutrition 54, 245S-
757 260S.
758 McDowell, F.W., McIntosh, W.C., Farley, K.A., 2005. A precise 40Ar–39Ar reference age
759 for the Durango apatite (U–Th)/He and fission-track dating standard. Chemical Geology
760 214, 249-263.
761 Muller, W., Shelley, M., Miller, P., Broude, S., 2009. Initial performance metrics of a new
762 custom-designed ArF excimer LA-ICPMS system coupled to a two-volume laser-
763 ablation cell. Journal of Analytical Atomic Spectrometry 24, 209-214.
764 Nagler, T.F., Eisenhauer, A., Muller, A., Hemleben, C., Kramers, J., 2000. The delta 44Ca-
765 temperature calibration on fossil and cultured Globigerinoides sacculifer: New tool for
766 reconstruction of past sea surface temperatures. Geochemistry Geophysics Geosystems 1.
767 Palacz, Z., 2004. Measurements of Calcium isotope ratios using a Collision Cell interfaced
768 multi-collector ICPMS, PP.2. GV Instruments.
769 Reynard, L., Pearson, J., Henderson, G., Hedges, R., 2013. CALCIUM ISOTOPES IN
770 JUVENILE MILK□CONSUMERS. Archaeometry 55, 946-957.
771 Reynard, L.M., Henderson, G.M., Hedges, R.E.M., 2010. Calcium isotope ratios in animal
772 and human bone. Geochimica Et Cosmochimica Acta 74, 3735-3750.
773 Reynard, L.M., Henderson, G.M., Hedges, R.E.M., 2011. Calcium isotopes in archaeological
774 bones and their relationship to dairy consumption. Journal of Archaeological Science 38,
775 657-664.
776 Rudge, J.F., Reynolds, B.C., Bourdon, B., 2009. The double spike toolbox. Chemical
777 Geology 265, 420-431.
778 Russell, W.A., Papanastassiou, D.A., Tombrello, T.A., 1978. Ca Isotope Fractionation on
779 Earth and Other Solar-System Materials. Geochimica Et Cosmochimica Acta 42, 1075-
780 1090.
781 Saggese, G., Baroncelli, G.I., Bertelloni, S., 2002. Puberty and bone development. Best
782 Practice & Research Clinical Endocrinology & Metabolism 16, 53-64.
783 Schiller, M., Paton, C., Bizzarro, M., 2012. Calcium isotope measurement by combined HR-
784 MC-ICPMS and TIMS. Journal of Analytical Atomic Spectrometry 27, 38-49.
785 Schiller., M., Daton., C., Bizzarro, M., 2012. Calcium isotope measurement by combined
786 HR-MC-ICPMS and TIMS. Journal of Analytical Atomic Spectrometry 27, 38-49.
787 Schmitt, A.D., Chabaux, F., Stille, P., 2003. The calcium riverine and hydrothermal isotopic
788 fluxes and the oceanic calcium mass balance. Earth and Planetary Science Letters 213,
789 503-518.

790 Skulan, J., Bullen, T., Anbar, A.D., Puzas, J.E., Shackelford, L., LeBlanc, A., Smith, S.M.,
791 2007. Natural calcium isotopic composition of urine as a marker of bone mineral balance.
792 Clinical Chemistry 53, 1155-1158.
793 Skulan, J., DePaolo, D.J., 1999. Calcium isotope fractionation between soft and mineralized
794 tissues as a monitor of calcium use in vertebrates. Proceedings of the National Academy
795 of Sciences 96, 13709-13713.
796 Skulan, J., DePaolo, D.J., Owens, T.L., 1997. Biological control of calcium isotopic
797 abundances in the global calcium cycle. Geochimica Et Cosmochimica Acta 61, 2505-
798 2510.
799 Smith, C., 1998. Cellular and chemical events during enamel maturation. Critical Reviews in
800 Oral Biology & Medicine 9, 128-161.
801 Tacail, T., Albalat, E., Telouk, P., Balter, V., 2014. A simplified protocol for measurement of
802 Ca isotopes in biological samples. Journal of Analytical Atomic Spectrometry 29, 529-
803 535.
804 Theintz, G., Buchs, B., Rizzoli, R., Slosman, D., Clavien, H., Sizonenko, P., Bonjour, J.-P.,
805 1992. Longitudinal monitoring of bone mass accumulation in healthy adolescents:
806 evidence for a marked reduction after 16 years of age at the levels of lumbar spine and
807 femoral neck in female subjects. The Journal of Clinical Endocrinology & Metabolism
808 75, 1060-1065.
809 Thompson, G., Anderson, D., Popovich, F., 1975. Sexual dimorphism in dentition
810 mineralization. Growth 39, 289-301.
811 Tipper, E., Galy, A., Bickle, M., 2006. Riverine evidence for a fractionated reservoir of Ca
812 and Mg on the continents: implications for the oceanic Ca cycle. Earth and Planetary
813 Science Letters 247, 267-279.
814 Tipper, E.T., Louvat, P., Capmas, F., Galy, A., Gaillardet, J., 2008. Accuracy of stable Mg
815 and Ca isotope data obtained by MC-ICP-MS using the standard addition method.
816 Chemical Geology 257, 65-75.
817 Uysal, T., Sari, Z., Ramoglu, S.I., Basciftci, F.A., 2004. Relationships between dental and
818 skeletal maturity in Turkish subjects. The Angle Orthodontist 74, 657-664.
819 Wieser, M.E., Buhl, D., Bouman, C., Schwieters, J., 2004. High precision calcium isotope
820 ratio measurements using a magnetic sector multiple collector inductively coupled
821 plasma mass spectrometer. Journal of Analytical Atomic Spectrometry 19, 844-851.
822 Young, E., Myers, A., Munson, E., Conklin, N.M., 1969. Mineralogy and geochemistry of
823 fluorapatite from Cerro de Mercado, Durango, Mexico. US Geological Survey
824 Professional Paper 650, D84-D93.
825 Zeng, D.L., Wu, Z.L., Cui, M.Y., 2010. Chronological age estimation of third molar
826 mineralization of Han in southern China. International Journal of Legal Medicine 124,
827 119-123.
828 Zhu, P., Macdougall, J.D., 1998. Calcium isotopes in the marine environment and the oceanic
829 calcium cycle. Geochimica Et Cosmochimica Acta 62, 1691-1698.

830

831

831 Table 1. Ca isotopic ratios and abundance of ^{42}Ca–^{48}Ca double spike (DS) solution. Note that
832 the isotopic abundances were calculated from the weights of each spike in the DS solution
833 and their certified values of abundance.

Isotopic ratios	**42-48Ca DS**		**Isotopic abundance* (%)**	**42-48Ca DS**
$^{40}Ca/^{44}Ca$	9.21970		^{40}Ca	3.331
$^{42}Ca/^{44}Ca$	99.0069		^{42}Ca	38.627
$^{43}Ca/^{44}Ca$	0.444707		^{43}Ca	0.128
$^{48}Ca/^{44}Ca$	131.851		^{44}Ca	0.112
$^{46}Ca/^{44}Ca$	<0.002		^{46}Ca	0.003
			^{48}Ca	57.803

834 .

835

836 Table 2. TIMS Ca isotopic ratios of standards SRM 915b, HPS_{new}, Fisher07, SRM 1486
837 (bone meal), and Durango apatite, internally-normalized to $^{42}Ca/^{44}Ca$ of 0.31221 (DePaolo,
838 2004).

	$^{40}Ca/^{44}Ca$	$^{43}Ca/^{44}Ca$	$^{46}Ca/^{44}Ca$	$^{48}Ca/^{44}Ca$
SRM 915b	47.164 ± 0.009	0.064865 ± 0.000005	0.001515 ± 0.000006	0.088687 ± 0.000031
HPS_{new}	47.160 ± 0.011	0.064866 ± 0.000005	0.001515 ± 0.000006	0.088684 ± 0.000036
Fisher07	47.165 ± 0.003	0.064868 ± 0.000002	0.001516 ± 0.000007	0.088688 ± 0.000004
Bone meal	47.162 ± 0.008	0.064868 ± 0.000004	0.001516 ± 0.000006	0.088694 ± 0.000033
Durango	47.161 ± 0.006	0.064866 ± 0.000005	0.001515 ± 0.00004	0.088716 ± 0.000066
Average	47.161 ± 0.011	0.064866 ± 0.000005	0.001515 ± 0.000006	0.088687 ± 0.000037

839

840

841 Table 3. The mean DS-corrected TIMS Ca isotopic ratios and $\delta^{44/40}Ca$ of the Ca isotopic
842 standards, relative to 915a.

	$^{40}Ca/^{44}Ca$	$^{42}Ca/^{44}Ca$	$^{48}Ca/^{44}Ca$	$\delta^{44}/^{40}Ca$ (‰) relative to 915a
SRM 915b	47.236 ± 0.011	0.312477 ± 0.000036	0.088585 ± 0.000019	0.72%
HPS_{new}	47.237 ± 0.008	0.312481 ± 0.000029	0.088583 ± 0.000015	0.70 ± 0.18
Fisher 07	47.221 ± 0.009	0.312432 ± 0.000041	0.088609 ± 0.000022	1.03 ± 0.20
Bone meal	47.318 ± 0.009	0.312744 ± 0.000028	0.088444 ± 0.000015	-1.03 ± 0.19
Durango	47.236 ± 0.008	0.312479 ± 0.000026	0.088584 ± 0.000014	0.70 ± 0.17

843

844 Table 4 TIMS Ca isotopic data of the laser-cut microsamples extracted from a lower left third
845 molar of a young Chinese female (CLW2). $^{40}Ca/^{44}Ca_T$, $^{48}Ca/^{44}Ca_T$ and $^{42}Ca/^{44}Ca_T$ are double
846 spike (DS) corrected ratios.

Microsamples	$^{40}Ca/^{44}Ca_T$	$^{48}Ca/^{44}Ca_T$	$^{42}Ca/^{44}Ca_T$	$\delta^{44/40}Ca$ (‰)
CLW2_1L	47.296 ± 0.002	0.088482 ± 0.000003	0.312670 ± 0.000007	-0.55 ± 0.04
CLW2_1R	47.270 ± 0.002	0.088526 ± 0.000003	0.312589 ± 0.000006	-0.02 ± 0.04
CLW2_2L	47.277 ± 0.002	0.088514 ± 0.000004	0.312612 ± 0.000007	-0.16 ± 0.05
CLW2_3L	47.287 ± 0.010	0.088497 ± 0.000017	0.312643 ± 0.000033	-0.37 ± 0.21
CLW2_3L_Re	47.301 ± 0.015	0.088473 ± 0.000025	0.312689 ± 0.000047	-0.67 ± 0.31
CLW2_2R	47.303 ± 0.002	0.088469 ± 0.000003	0.312696± 0.000005	-0.71 ± 0.03
CLW2_4R	47.277 ± 0.004	0.088515 ± 0.000006	0.312610 ± 0.000012	-0.15 ± 0.08
CLW2_4R Re	47.277 ± 0.002	0.088515 ± 0.000004	0.312609 ± 0.000007	-0.15 ± 0.05
CLW2_5R	47.269 ± 0.005	0.088529 ± 0.000009	0.312584 ± 0.000017	0.02 ± 0.11
CLW2_5R_Re	47.268 ± 0.002	0.088529 ± 0.000004	0.312582 ± 0.000008	0.03 ± 0.05
CLW2_6R	47.285 ± 0.002	0.088500 ± 0.000004	0.312637 ± 0.000007	-0.33 ± 0.05

847

848

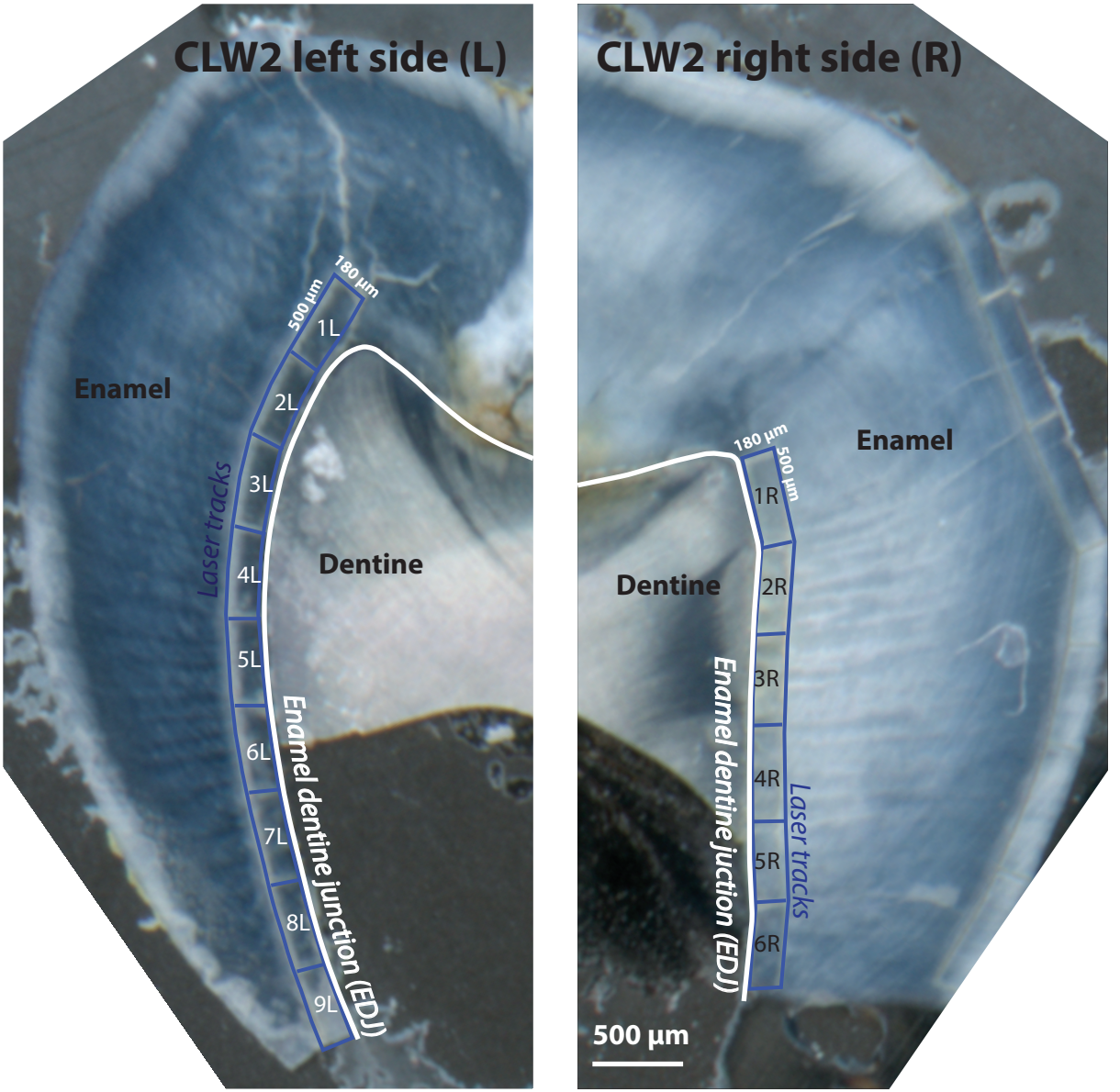
CLW2 left side (L)
Enamel
Dentine
Laser tracks
Enamel dentine junction (EDJ)
180 µm
500 µm
1L
2L
3L
4L
5L
6L
7L
8L
9L
CLW2 right side (R)
Enamel
Dentine
Enamel dentine junction (EDJ)
Laser tracks
180 µm
500 µm
1R
2R
3R
4R
5R
6R
500 µm

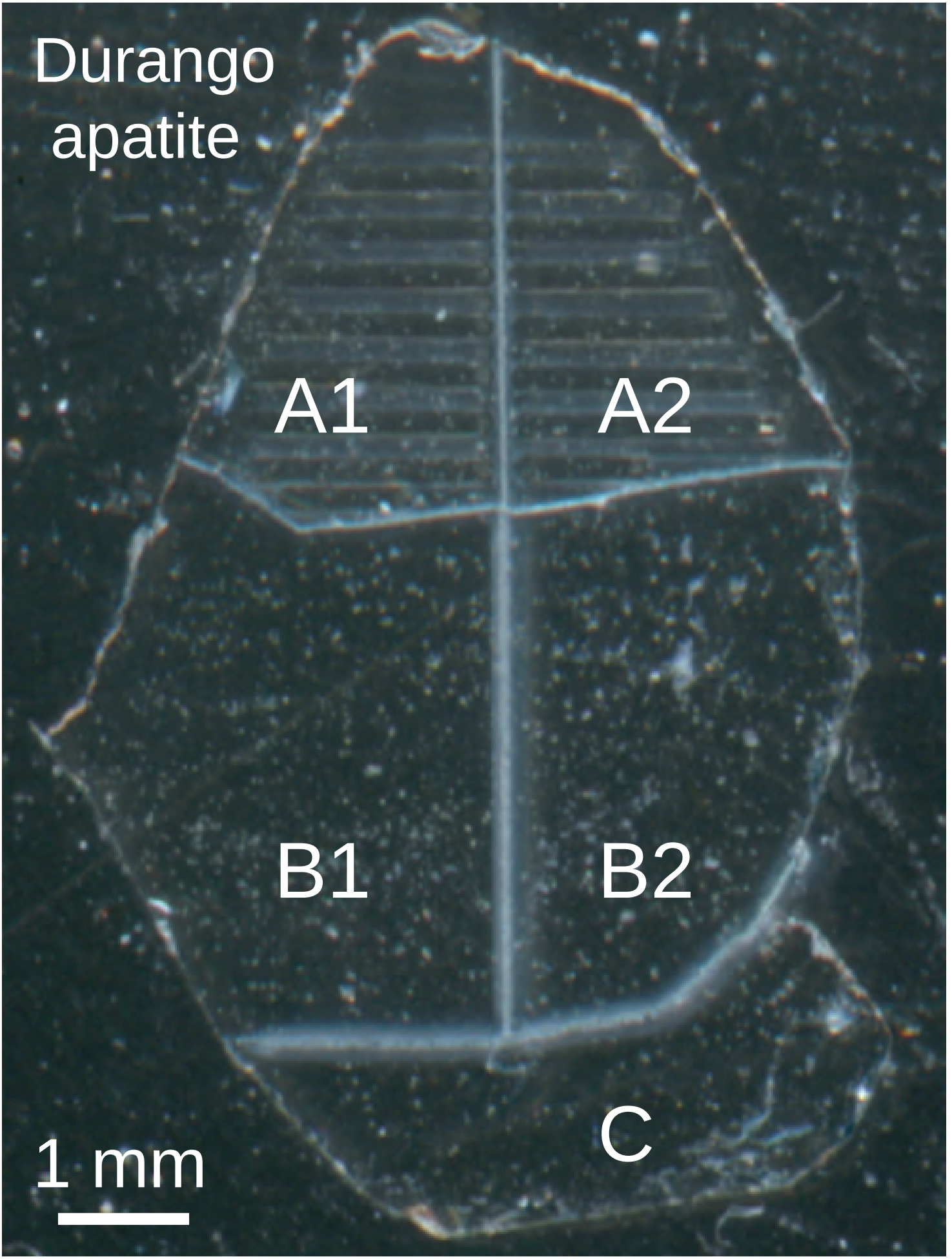
Durango
apatite
A1
A2
B1
B2
C
1 mm

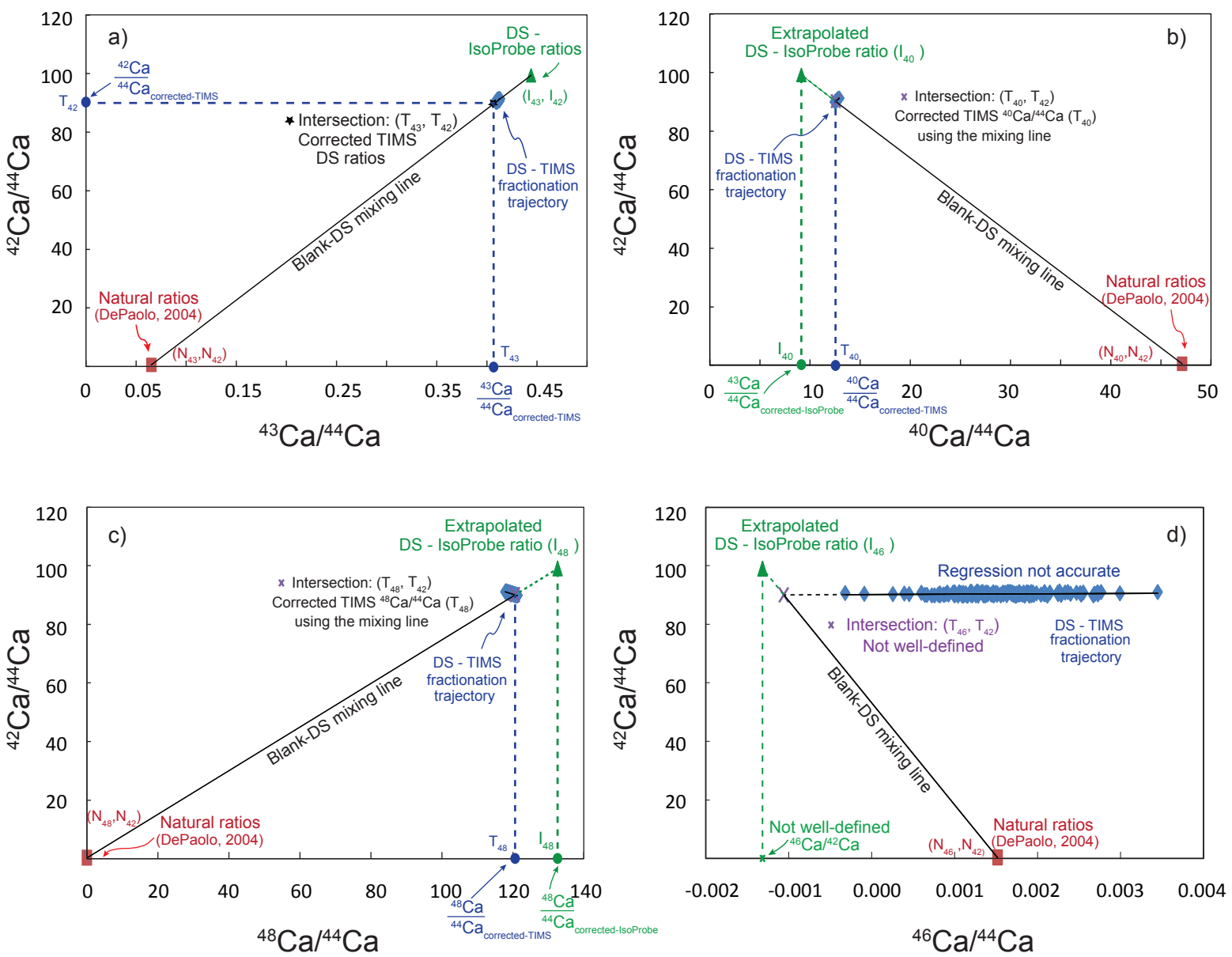
a)
DS - IsoProbe ratios
$\frac{^{42}Ca}{^{44}Ca}_{corrected\text{-}TIMS}$
T_{42}
(I_{43}, I_{42})
Intersection: (T_{43}, T_{42})
Corrected TIMS DS ratios
DS - TIMS fractionation trajectory
Blank-DS mixing line
Natural ratios (DePaolo, 2004)
(N_{43},N_{42})
T_{43}
$^{42}Ca/^{44}Ca$
$^{43}Ca/^{44}Ca$
b)
Extrapolated DS - IsoProbe ratio (I_{40})
Intersection: (T_{40}, T_{42})
Corrected TIMS $^{40}Ca/^{44}Ca$ (T_{40}) using the mixing line
DS - TIMS fractionation trajectory
Blank-DS mixing line
Natural ratios (DePaolo, 2004)
I_{40}
T_{40}
(N_{40},N_{42})
$\frac{^{43}Ca}{^{44}Ca}_{corrected\text{-}IsoProbe}$
$\frac{^{40}Ca}{^{44}Ca}_{corrected\text{-}TIMS}$
$^{42}Ca/^{44}Ca$
$^{40}Ca/^{44}Ca$
c)
Extrapolated DS - IsoProbe ratio (I_{48})
Intersection: (T_{48}, T_{42})
Corrected TIMS $^{48}Ca/^{44}Ca$ (T_{48}) using the mixing line
DS - TIMS fractionation trajectory
Blank-DS mixing line
(N_{48},N_{42})
Natural ratios (DePaolo, 2004)
T_{48}
I_{48}
$\frac{^{48}Ca}{^{44}Ca}_{corrected\text{-}TIMS}$
$\frac{^{48}Ca}{^{44}Ca}_{corrected\text{-}IsoProbe}$
$^{42}Ca/^{44}Ca$
$^{48}Ca/^{44}Ca$
d)
Extrapolated DS - IsoProbe ratio (I_{46})
Regression not accurate
Intersection: (T_{46}, T_{42})
Not well-defined
DS - TIMS fractionation trajectory
Blank-DS mixing line
Not well-defined $^{46}Ca/^{42}Ca$
(N_{46},N_{42})
Natural ratios (DePaolo, 2004)
$^{42}Ca/^{44}Ca$
$^{46}Ca/^{44}Ca$

915b HPS$_{new}$ Fisher07 Durango apatite Bone meal

$^{40}Ca/^{44}Ca$ norm

47.180
47.170
47.160
47.150
47.140

$^{43}Ca/^{44}Ca$ norm

0.06488
0.06487
0.06486
0.06485

$^{48}Ca/^{44}Ca$ norm

0.08872
0.08868
0.08864

45.0 45.5 46.0 46.5 47.0 47.5 48.0

$^{40}Ca/^{44}Ca$ measured

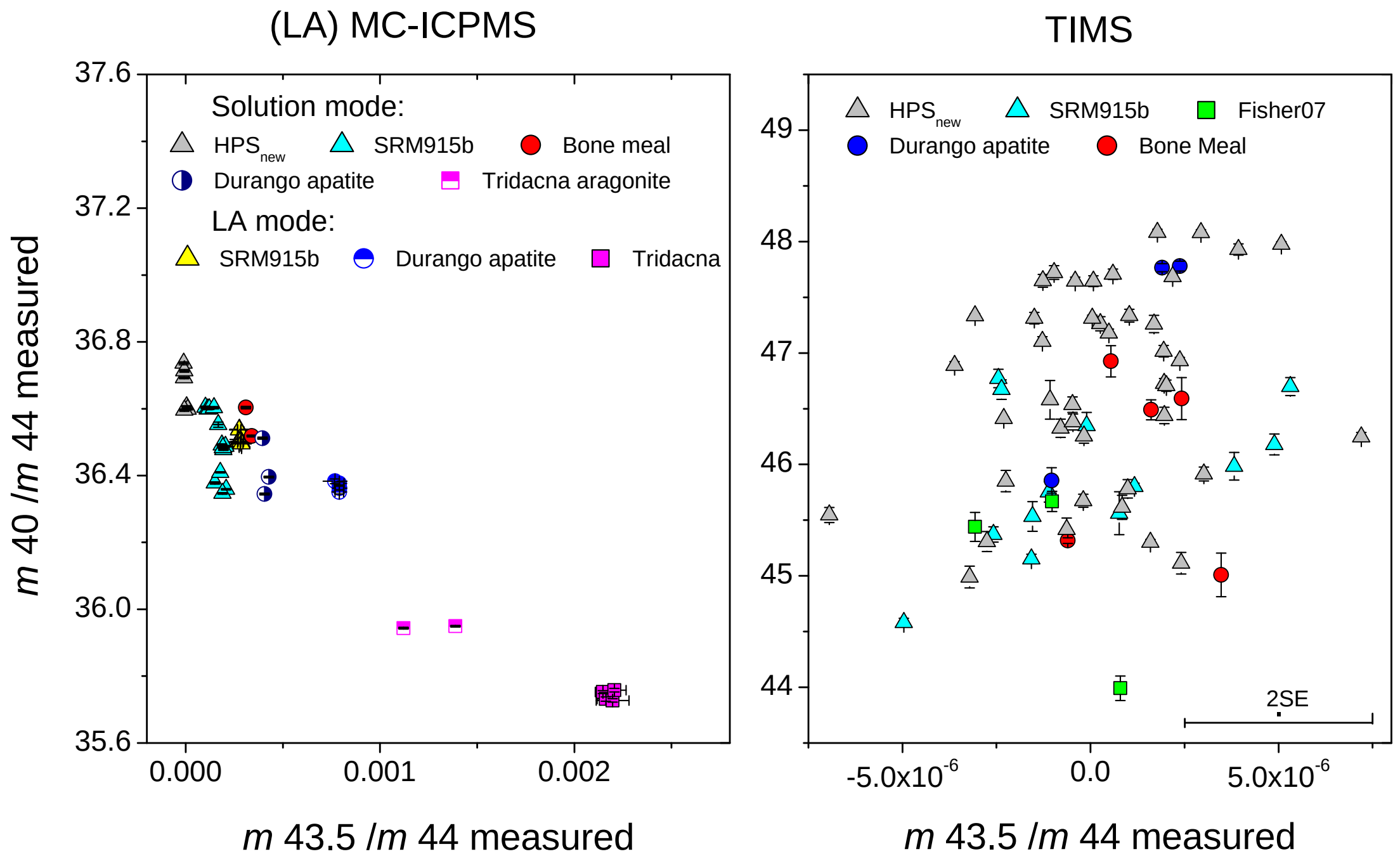
(LA) MC-ICPMS
TIMS
Solution mode:
HPS new
SRM915b
Bone meal
Durango apatite
Tridacna aragonite
LA mode:
SRM915b
Durango apatite
Tridacna
HPS new
SRM915b
Fisher07
Durango apatite
Bone Meal
2SE
m 40 /m 44 measured
m 43.5 /m 44 measured
m 43.5 /m 44 measured
37.6
37.2
36.8
36.4
36.0
35.6
0.000
0.001
0.002
49
48
47
46
45
44
-5.0x10-6
0.0
5.0x10-6

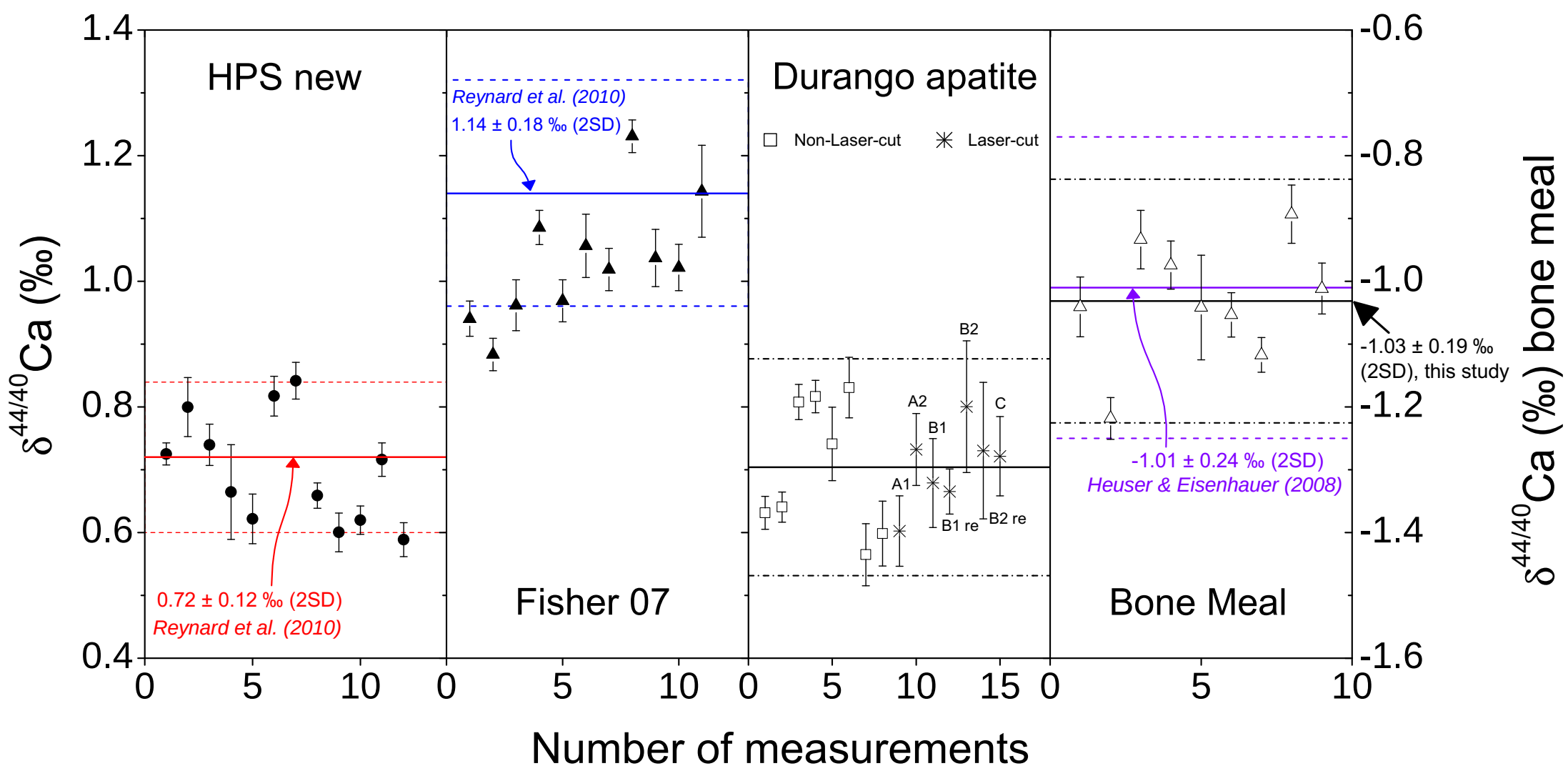
HPS new
Fisher 07
Durango apatite
Bone Meal
Non-Laser-cut
Laser-cut
Reynard et al. (2010)
1.14 ± 0.18 ‰ (2SD)
0.72 ± 0.12 ‰ (2SD)
Reynard et al. (2010)
-1.03 ± 0.19 ‰
(2SD), this study
-1.01 ± 0.24 ‰ (2SD)
Heuser & Eisenhauer (2008)
A1
A2
B1
B1 re
B2
B2 re
C
δ44/40Ca (‰)
δ44/40Ca (‰) bone meal
Number of measurements

SRM 915b
Tridacna aragonite
Durango apatite
$^{42}Ca/^{44}Ca$ M
0.2770
0.2768
0.2766
0.2764
$^{43}Ca/^{44}Ca$ M
0.06117
0.06114
0.06111
0.06108
$^{40}Ca/^{44}Ca$ M
36.760
36.720
36.680
36.640
36.600
0
2
4
6
8
10
12
14
16
18
Analytical number

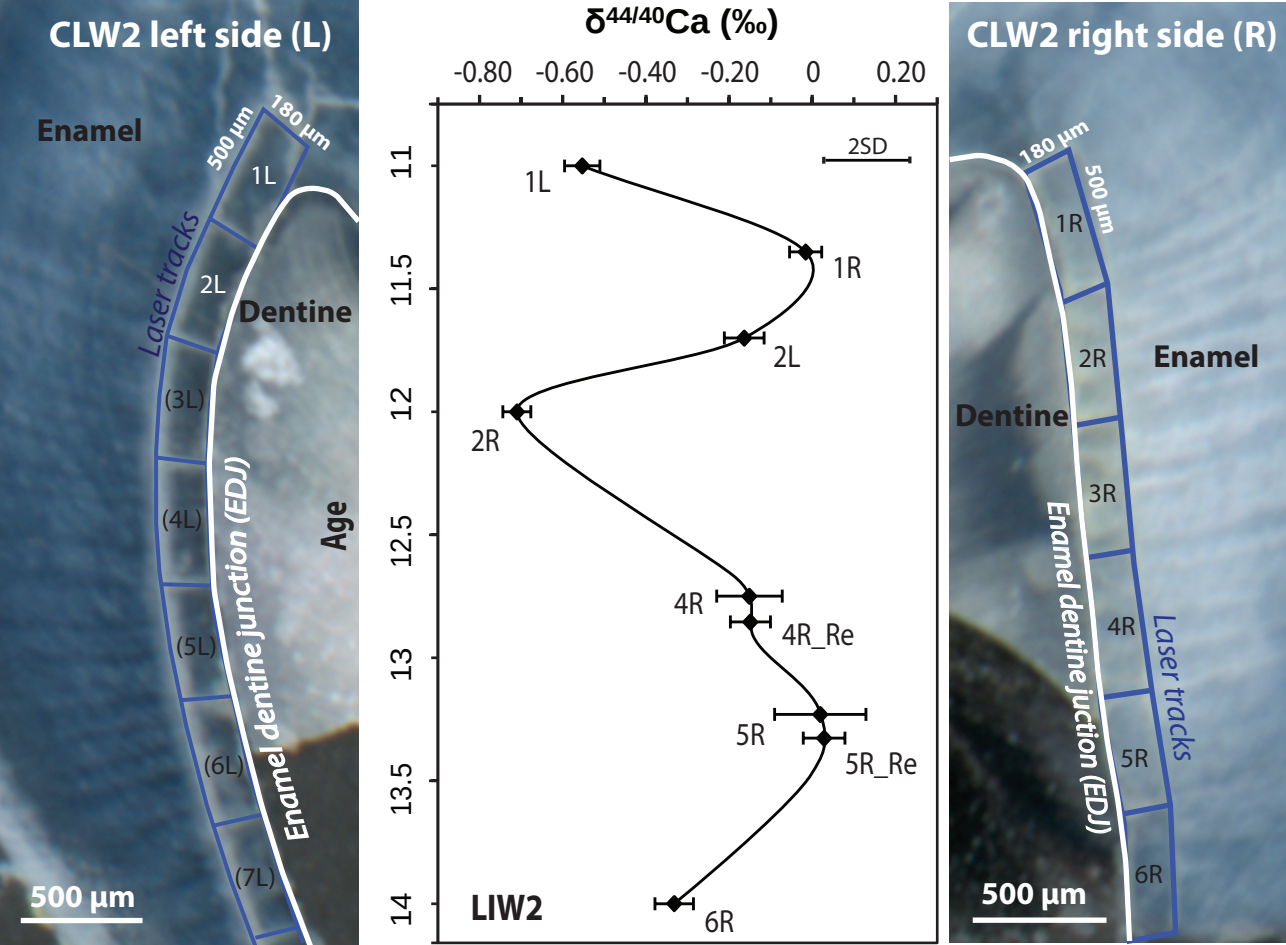
CLW2 left side (L)
Enamel
500 µm
180 µm
1L
Laser tracks
2L
Dentine
(3L)
(4L)
Age
(5L)
Enamel dentine junction (EDJ)
(6L)
(7L)
500 µm
δ44/40Ca (‰)
-0.80 -0.60 -0.40 -0.20 0 0.20
11
11.5
12
12.5
13
13.5
14
2SD
1L
1R
2L
2R
4R
4R_Re
5R
5R_Re
6R
LIW2
CLW2 right side (R)
180 µm
500 µm
1R
2R
Enamel
Dentine
3R
Enamel dentine juction (EDJ)
4R
Laser tracks
5R
6R
500 µm

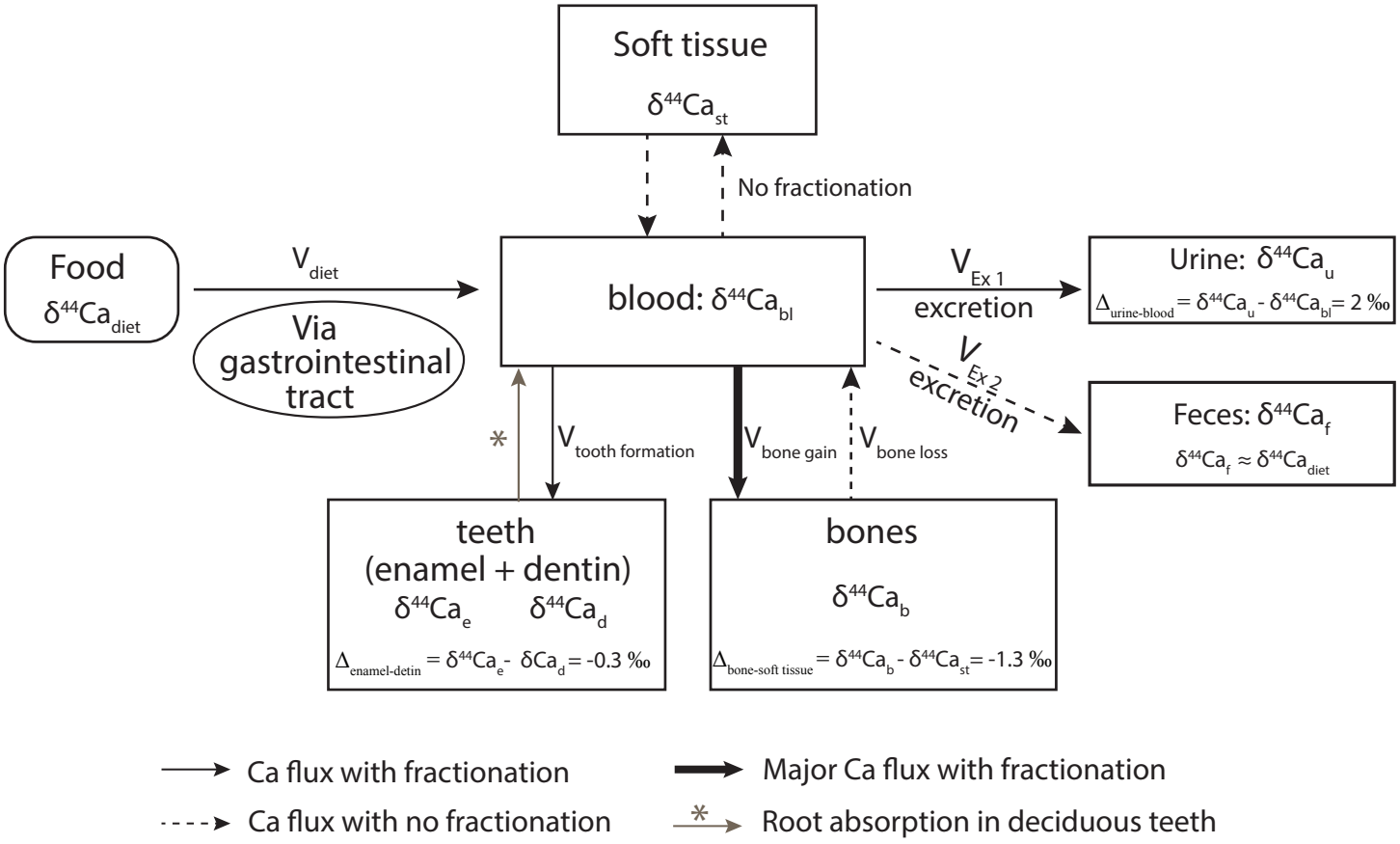
Soft tissue
δ44Cast
No fractionation
Food
δ44Cadiet
Vdiet
Via gastrointestinal tract
blood: δ44Cabl
VEx 1 excretion
Urine: δ44Cau
Δurine-blood = δ44Cau - δ44Cabl = 2 ‰
VEx 2 excretion
Feces: δ44Caf
δ44Caf ≈ δ44Cadiet
*
Vtooth formation
Vbone gain
Vbone loss
teeth
(enamel + dentin)
δ44Cae δ44Cad
Δenamel-detin = δ44Cae - δCad = -0.3 ‰
bones
δ44Cab
Δbone-soft tissue = δ44Cab - δ44Cast = -1.3 ‰
Ca flux with fractionation
Major Ca flux with fractionation
Ca flux with no fractionation
* Root absorption in deciduous teeth